Thymic progenitor homing and lymphocyte homeostasis are linked via S1P-controlled expression of thymic P-selectin/CCL25

Klaus Gossens,[1] Silvia Naus,[1] Stephane Y. Corbel,[1] Shujun Lin,[1] Fabio M.V. Rossi,[1,2] Jürgen Kast,[1,3] and Hermann J. Ziltener[1,4]

[1]The Biomedical Research Centre, [2]Department of Medical Genetics, [3]Department of Chemistry, and [4]Department of Pathology and Laboratory Medicine, University of British Columbia, Vancouver, British Columbia V6T 1Z3, Canada

Thymic T cell progenitor (TCP) importation is a periodic, gated event that is dependent on the expression of functional P-selectin ligands on TCPs. Occupancy of intrathymic TCP niches is believed to negatively regulate TCP importation, but the nature of this feedback mechanism is not yet resolved. We show that P-selectin and CCL25 are periodically expressed in the thymus and are essential parts of the thymic gate-keeping mechanism. Periodicity of thymic TCP receptivity and the size of the earliest intrathymic TCP pool were dependent on the presence of functional P-selectin ligand on TCPs. Furthermore, we show that the numbers of peripheral blood lymphocytes directly affected thymic P-selectin expression and TCP receptivity. We identified sphingosine-1-phosphate (S1P) as one feedback signal that could mediate influence of the peripheral lymphocyte pool on thymic TCP receptivity. Our findings suggest a model whereby thymic TCP importation is controlled by both early thymic niche occupancy and the peripheral lymphocyte pool via S1P.

CORRESPONDENCE
Hermann J. Ziltener:
hermann@brc.ubc.ca

Abbreviations used: ATF, activating transcription factor; C2GnT1, core 2 β1,6-glucosaminyltransferase-I; DOP, 2-deoxypyridoxine; DP, double positive; ETP, early TCP; HDL, high-density lipoprotein; ICAM-1, intercellular adhesion molecule 1; LC-MS/MS, liquid chromatography–mass spectrometry/mass spectrometry; PSGL-1, P-selectin glycoprotein ligand 1; qrtPCR, quantitative real-time PCR; S1P, sphingosine-1-phosphate; S1PR, S1P receptor; SP, single positive; TCP, T cell progenitor; TREC, T cell receptor excision circle; TN, triple negative; VCAM-1, vascular cell adhesion molecule 1; VE-cadherin, vascular endothelial–cadherin.

The thymus does not contain self-renewing T cell progenitors (TCPs) and, therefore, requires continuous importation of progenitors from the blood to sustain T cell output (1, 2). Recruitment of TCPs to the thymus is facilitated by a multistep adhesion cascade initiated by the interaction of P-selectin glycoprotein ligand 1 (PSGL-1) expressed on TCPs, with P-selectin (CD62P) expressed on thymic endothelium (3, 4). Specific N-terminal carbohydrate modifications on PSGL-1 catalyzed by glycosyltransferases are required for binding to P-selectin. In particular, the activity of the core 2 β1,6-glucosaminyltransferase-I (C2GnT1) has been highlighted in selectin ligand formation on PSGL-1 (5). Interaction of PSGL-1 with endothelial P-selectin slows down TCPs, and allows them to respond to local chemokine gradients and to engage the endothelial adhesion molecules intercellular adhesion molecule 1 (ICAM-1) and vascular cell adhesion molecule 1 (VCAM-1) via integrins, leading to a firm arrest of TCPs on the thymic endothelium (4).

Thymic TCP importation is independent of the numbers of available TCPs in the blood (6) and is not a steady-state process, as the thymus alternates between nonreceptive and receptive periods (2). This suggests that a feedback mechanism regulates expression of recruitment signals on vascular or perivascular cells. One factor proposed to control progenitor entry into the thymus is the limited availability of intrathymic niches for which TCPs compete and, thus, gain access to survival and differentiation factors necessary for their development (6). Full thymic niches are thought to trigger a feedback signal to reduce TCP importation, but the nature of these feedback signals and how they influence thymic TCP entry is unknown.

To explore the basis of feedback signals that determine periodicity in thymic TCP receptivity, we analyzed the expression of adhesion molecules in WT mice and mouse strains with distinct thymic receptivities. We found that thymic P-selectin and CCL25 expression correlated with thymic TCP receptivity, suggesting that these molecules function as thymic gatekeepers. Furthermore, we found that P-selectin expression and thymic TCP receptivity correlated inversely

The Rockefeller University Press $30.00
J. Exp. Med. Vol. 206 No. 4 761-778
www.jem.org/cgi/doi/10.1084/jem.20082502

with peripheral lymphocyte numbers and could be manipulated by experimentally altering peripheral lymphocyte numbers. These results show that the peripheral lymphocyte pool feeds back to thymic TCP entry sites and modifies thymic TCP importation by regulating P-selectin and CCL25 expression.

RESULTS

Thymi of PSGL-1$^{-/-}$ and IL-7R$\alpha^{-/-}$ mice are hyperreceptive for TCPs

We showed previously that P-selectin is functionally involved in thymic TCP importation and that thymic P-selectin RNA expression reversely correlated with thymic niche occupancy status (3). To further characterize the relationship of thymic P-selectin expression and TCP receptivity, we used two complementary approaches to assess thymic TCP receptivity in mice deficient for IL-7Rα, RAG-1, C2GnT1, PSGL-1, or Psel. Short-term homing assays were performed to determine the capacity of thymi to import i.v. injected CFSE-labeled bone marrow cells from the blood stream. Long-term reconstitutions of nonirradiated hosts were performed to determine the contribution of i.v. injected bone marrow cells to the host's double-positive (DP) thymocyte pool.

Short-term receptivity of thymi was expressed as a ratio of homed cells to thymic cell numbers (Fig. 1, a and b), or per milligram of thymic weight (Fig. 1 c), to eliminate a skewing of the data because of variations in thymic size in the different mouse strains analyzed (Fig. S1). When expressed as ratio of the number of homed CFSE$^+$ cells per 2×10^6 thymocytes, our data show that IL-7R$^{-/-}$ thymi import fourfold more CFSE$^+$ cells than WT mice (Fig. 1 a). PSGL-1$^{-/-}$ mice also show significantly increased receptivity for CFSE$^+$ bone marrow cells, whereas C2GnT1$^{-/-}$ thymi did not show an increased receptivity when compared with WT mice. Receptivity in RAG-1$^{-/-}$ thymi was nonsignificantly reduced compared with WT mice.

Short-term homing data displayed as a ratio of homed lineage marker (Lin: CD3, CD4, CD8, CD19, Gr-1, CD11b, CD11c, Ter119, NK, and γ/δTCR)–negative CFSE$^+$ cells per 2×10^6 thymocytes demonstrated that IL-7R$^{-/-}$ mice showed an almost 30-fold increased thymic receptivity compared with WT mice (Fig. 1 b); PSGL-1$^{-/-}$ and C2GnT1$^{-/-}$ mice had an 8- and 2-fold increased receptivity, respectively, whereas receptivity in RAG-1$^{-/-}$ mice was reduced. When data were expressed as numbers of CFSE$^+$ cells per milligram of thymic tissue, IL-7R$^{-/-}$ thymi were again found to be the most receptive, with $\sim$80 CFSE$^+$ cells per milligram of thymus, followed by PSGL-1$^{-/-}$ and C2GnT1$^{-/-}$ thymi, with 60 and 40 CFSE$^+$ cells per milligram of thymic tissue, respectively (Fig. 1 c). In contrast, RAG-1$^{-/-}$ mice showed significantly ($P < 0.001$) reduced receptivity when compared with WT controls. The numbers of CFSE$^+$ cells per milliliter of blood was similar in all mouse strains, confirming that differences in thymic importation are not caused by differences of injected donor cells in the blood (Fig. 1 d). Collectively, this set of data shows that IL-7R$^{-/-}$ and PSGL-1$^{-/-}$ thymi have increased receptivity, whereas C2GnT1$^{-/-}$ mice showed no or only modest increased thymic receptivity. In contrast, RAG-1$^{-/-}$ thymi had a reduced receptivity.

The short-term assay cannot be used to determine whether the thymi import truly functional TCPs to various degrees, because neither the exact nature of the TCP population in the blood that seeds the thymus under physiological conditions nor the intrathymic TCP population that contributes predominantly to T cell formation is yet known (7). Long-term thymus reconstitution experiments in nonirradiated recipients were thus used to evaluate whether the observed increased short-term receptivity in IL-7R$^{-/-}$ and PSGL-1$^{-/-}$ mice corresponded to an increased contribution of injected donor bone marrow to thymocyte formation. 3 wk after bone marrow transfer, the long-term reconstitution experiments showed that IL-7R$^{-/-}$ mice had the highest chimerism (79×10^6 donor-derived DP thymocytes), and that there was a significant increase in the numbers of donor-derived DP thymocytes in PSGL-1$^{-/-}$ and C2GnT1$^{-/-}$ mice (38×10^6 and 20×10^6, respectively) when compared with WT recipients (4.2×10^6 donor-derived DP thymocytes; Fig. 1 e), whereas thymi of RAG-1$^{-/-}$ mice had significantly lower numbers (4.4×10^5) of donor-derived DP thymocytes (Fig. 1 e), in agreement with the data from the short-term homing assays.

P-selectin and CCL25 expression correlate with thymic TCP importation

To determine whether differences in thymic P-selectin expression could explain differences in thymic receptivity, we measured P-selectin RNA expression by quantitative real-time PCR (qrtPCR) on whole thymic tissues. Thymic P-selectin expression is restricted to endothelial cells (3). Thus, P-selectin RNA was normalized using the endothelial-specific marker vascular endothelial–cadherin (VE-cadherin) to exclude a skewing of the data because of differences in thymic size and relative endothelial content. P-selectin RNA levels were high in IL-7R$^{-/-}$ and PSGL-1$^{-/-}$ thymi when compared with WT thymi (Fig. 2 a). P-selectin RNA levels were also increased in C2GnT1$^{-/-}$ thymi but were $\sim$4.5-fold lower than in PSGL-1$^{-/-}$ thymi, whereas RAG-1$^{-/-}$ mice had significantly reduced thymic P-selectin RNA. Control experiments showed that P-selectin RNA levels in spleens were comparable in all mouse strains, demonstrating that altered P-selectin expression was thymus specific (Fig. 2 b).

To confirm that increased P-selectin RNA levels are associated with elevated P-selectin protein levels on thymic endothelial cells, we analyzed thymic endothelial cells (CD45$^-$, CD31$^+$, CD144$^+$) by flow cytometry. PSGL-1$^{-/-}$ and IL-7R$^{-/-}$ mice had a two- and fourfold increased frequency of Psel^{hi}-expressing endothelial cells, respectively, when compared with WT controls (Fig. 2 c). In C2GnT1$^{-/-}$ thymi, P-selectin protein expression was comparable to WT controls, whereas it was significantly reduced on endothelial cells from RAG-1$^{-/-}$ thymi.

In addition to P-selectin, the integrin ligands ICAM-1 and VCAM-1 and the chemokine CCL25 are known to support thymic TCP importation (4). To assess whether expression of

these molecules is similarly regulated to P-selectin expression, we compared RNA levels in the thymi of WT and the previously mentioned mouse strains. We found significantly increased levels of CCL25 RNA in the thymi of IL-7R$^{-/-}$ and PSGL-1$^{-/-}$ mice and, to a lower degree, in the thymi of Psel$^{-/-}$ mice when compared with WT thymi (Fig. 3 a). C2GnT1$^{-/-}$ mice showed similar CCL25 expression as WT mice. ICAM-1 and VCAM-1 RNA levels were comparable in all tested strains.

qrtPCR analysis performed on sorted thymic endothelial, cortical epithelial, and medullary epithelial cells confirmed that P-selectin and the reference gene VE-cadherin were exclusively expressed in thymic endothelial cells (CD45^{-}, CD31^{+}, CD144^{+}) and were absent in cortical epithelial cells (CD45^{-}, Ly51^{hi}, G8.8^{+}) or medullary epithelial cells (CD45^{-}, Ly51^{int}, G8.8^{+}; Fig. 3 b). ICAM-1 and VCAM-1 were expressed in endothelial and epithelial cells. ICAM-1 was expressed highest

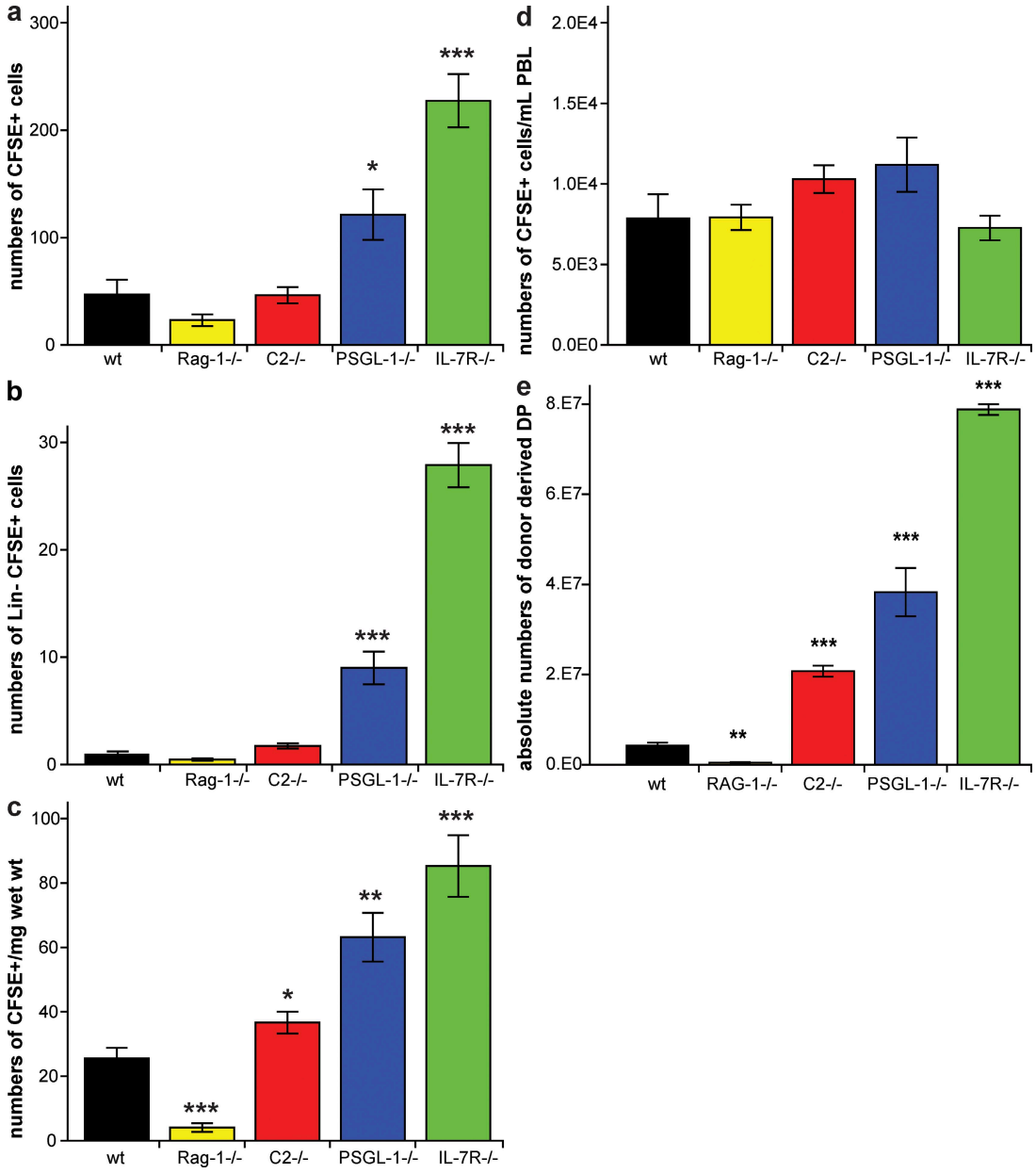

Figure 1. Thymic receptivity in WT, RAG-1$^{-/-}$, C2GnT1$^{-/-}$, PSGL-1$^{-/-}$, and IL-7R$^{-/-}$ mice in short- and long-term reconstitution assays. (a–d) 24 h after i.v. injection of CFSE-labeled nonfractionated bone marrow cells, mice were sacrificed, and thymi and peripheral blood (PBL) were analyzed for CFSE^{+} cells. (a) Absolute numbers of CFSE^{+} cells per 2 × 10^{6} thymocytes recovered from the thymi of the indicated mouse strains. (b) Absolute numbers of Lin^{-}CFSE^{+} cells per 2 × 10^{6} thymocytes recovered from thymi of the indicated mouse strains. (c) Absolute numbers of CFSE^{+} cells per milligram of thymus weight (wet wt) of the indicated mouse strains. (d) Absolute numbers of CFSE^{+} cells present in 1 ml PBL in the indicated mouse strains. (e) Absolute numbers of donor-derived DP thymocytes 3 wk after i.v. injection of congenic bone marrow into the indicated mouse strains. Data are representative of three independent experiments with at least six mice per group (means ± SEM). Mice were sex matched and 35 ± 3 d old. C2, C2GnT1. *, P < 0.05; **, P < 0.01; and ***, P < 0.001.

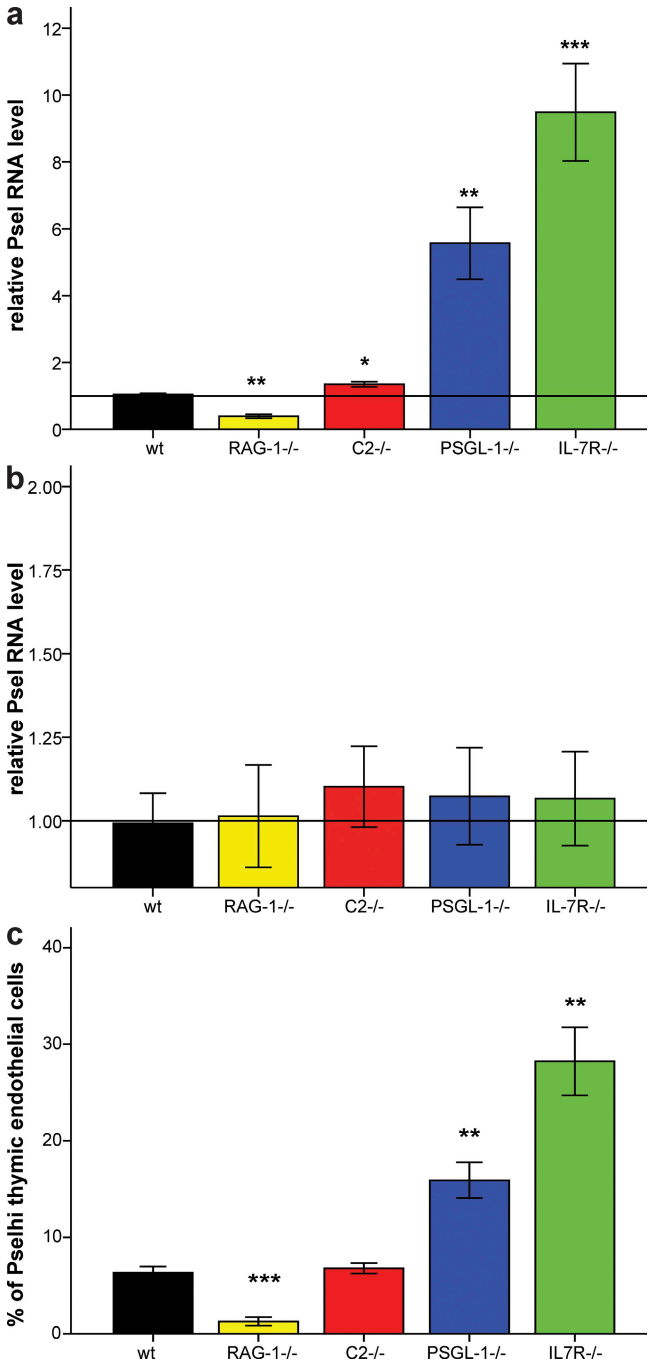

Figure 2. Thymic P-selectin expression is increased in hyperreceptive thymi of IL-7R$^{-/-}$ and PSGL-1$^{-/-}$ mice. P-selectin RNA expression determined by qrtPCR in (a) thymi and (b) spleens of mice of the indicated mouse strains. RNA levels were normalized to VE-cadherin expression and expressed relative to WT (=1, as indicated). (c) Frequencies of Psel^{hi}-expressing cells within the thymic endothelial cell population (defined as CD45$^-$, CD144$^+$, CD31$^+$) in thymic cell suspensions derived from WT, RAG-1$^{-/-}$, C2GnT1$^{-/-}$, PSGL-1$^{-/-}$, and IL-7R$\alpha^{-/-}$ mice, as determined by flow cytometry. Data are representative of three independent experiments with at least six mice per group in a and b, and at least three mice per group in c (means ± SEM). Mice were sex matched and 37 ± 2 d old. C2, C2GnT1. *, $P < 0.05$; **, $P < 0.01$; and ***, $P < 0.001$.

in endothelial cells, whereas the highest VCAM-1 expression was found in medullary epithelial cells. Furthermore, we found that CCL25 RNA levels were highest in endothelial cells, followed by medullary epithelial and cortical epithelial cells. Because the numbers of endothelial cells in the thymi of the different mouse strains were comparable (Fig. 3 c), skewing of our data caused by variations in thymic cell composition can be excluded.

Collectively, our data demonstrate that thymi with high receptivity for TCPs express elevated levels of P-selectin and CCL25, supporting the idea that these molecules are not only functionally involved in thymic TCP importation but might also be involved in regulating this process by differential expression.

P-selectin/CCL25 RNA is expressed periodically over time in WT but not in PSGL-1$^{-/-}$ or C2GnT1$^{-/-}$ thymi

Thymic progenitor importation periodically alternates between nonreceptive and receptive phases (2). Should P-selectin and CCL25 regulate TCP entry, we would expect these molecules to be expressed in an oscillating manner. We determined thymic P-selectin and CCL25 RNA expression in mice ranging in age from 12 to 68 d. In WT mice, P-selectin RNA expression was periodic, whereas P-selectin RNA levels remained relatively constant over time in C2GnT1$^{-/-}$ and PSGL-1$^{-/-}$ mice (Fig. 4, a–c). P-selectin RNA baseline levels were only slightly increased in C2GnT1$^{-/-}$ mice (1.5-fold) compared with 20-d-old WT controls but were significantly increased (4-fold) in PSGL-1$^{-/-}$ thymi. P-selectin expression in the spleens of WT, PSGL-1$^{-/-}$, or C2GnT1$^{-/-}$ mice remained relatively constant over time, suggesting that the observed periodicity is specific for the WT thymus (Fig. S2). In WT mice, the temporal thymic expression pattern of CCL25 RNA was similar to that observed for P-selectin (Fig. 4 d). Plotting the mean expression level of P-selectin as a function of mean CCL25 level at the same time points showed that P-selectin RNA expression highly correlated with CCL25 expression ($P < 0.001$; Pearson's $\rho = 0.607$; Fig. 4 e). Thymic CCL25 RNA expression again lacked periodicity in C2GnT1$^{-/-}$ and PSGL-1$^{-/-}$ mice, where it was expressed at relatively constant levels with only minor periodic changes. Similar to the observation for thymic P-selectin, CCL25 RNA levels were considerably higher in PSGL-1$^{-/-}$ thymi than in C2GnT1$^{-/-}$ thymi (Fig. 4 f).

Thymic niche occupancy is not the only factor limiting thymic receptivity

We next sought to identify the feedback signals that regulate thymic P-selectin/CCL25 expression and thymic TCP receptivity. It has been shown that competition for intrathymic niches, especially at the triple-negative (TN; all are Lin^{lo}CD4$^-$CD8$^-$, with TN1 CD44$^+$CD25$^-$, TN2 CD44$^-$CD25$^+$, and pre-DP CD44$^-$CD25$^-$) TN2 and TN3 stages, limits TCP entry into the thymus (8). To test this model, we reconstituted nonirradiated IL-7R$^{-/-}$ mice with FACS-sorted TN1, TN2, or TN3 WT thymocytes and measured thymic P-selectin expression and chimerism in the thymus and blood 12 d later

(Fig. 5 a; and Fig. S3, a and b). Injection with each TN subset led to thymic reconstitution and the formation of peripheral T cells (Fig. S3, a, d, and e), which was accompanied by a significant reduction in thymic P-selectin RNA when compared with the vehicle-treated controls (Fig. 5 a). TN3 cells did not give rise to TN1 or TN2 cells (Fig. S3 c), indicating that TN3 cells and their progeny are sufficient to control thymic receptivity. These data are consistent with the niche occupancy model, and we thus expected that the differences in thymic receptivities that we observed in our study were also caused by differences in thymic niche occupancy. We therefore compared content and distribution of thymocyte subsets in WT, PSGL-$1^{-/-}$, C2GnT$1^{-/-}$, and Psel$^{-/-}$ thymi. TN thymocyte subset distributions were surprisingly similar in WT and all three knockout strains (Fig. 5 b). However, the size of the early TCP (ETP; Lin^{lo}, $CD117^{hi}$, Sca-1^{+}, $CD44^{+}$, $CD25^{-}$) (9) population that is believed to contain the earliest intrathymic TCPs was reduced by 45–85% in the thymi of C2GnT$1^{-/-}$, PSGL-$1^{-/-}$, and Psel$^{-/-}$ mice (Fig. 5 c). Given that the total thymic cellularity and the numbers of thymocyte subsets in knockout thymi are similar to WT thymi (Fig. S1), we hypothesized that the size of intrathymic niches may be

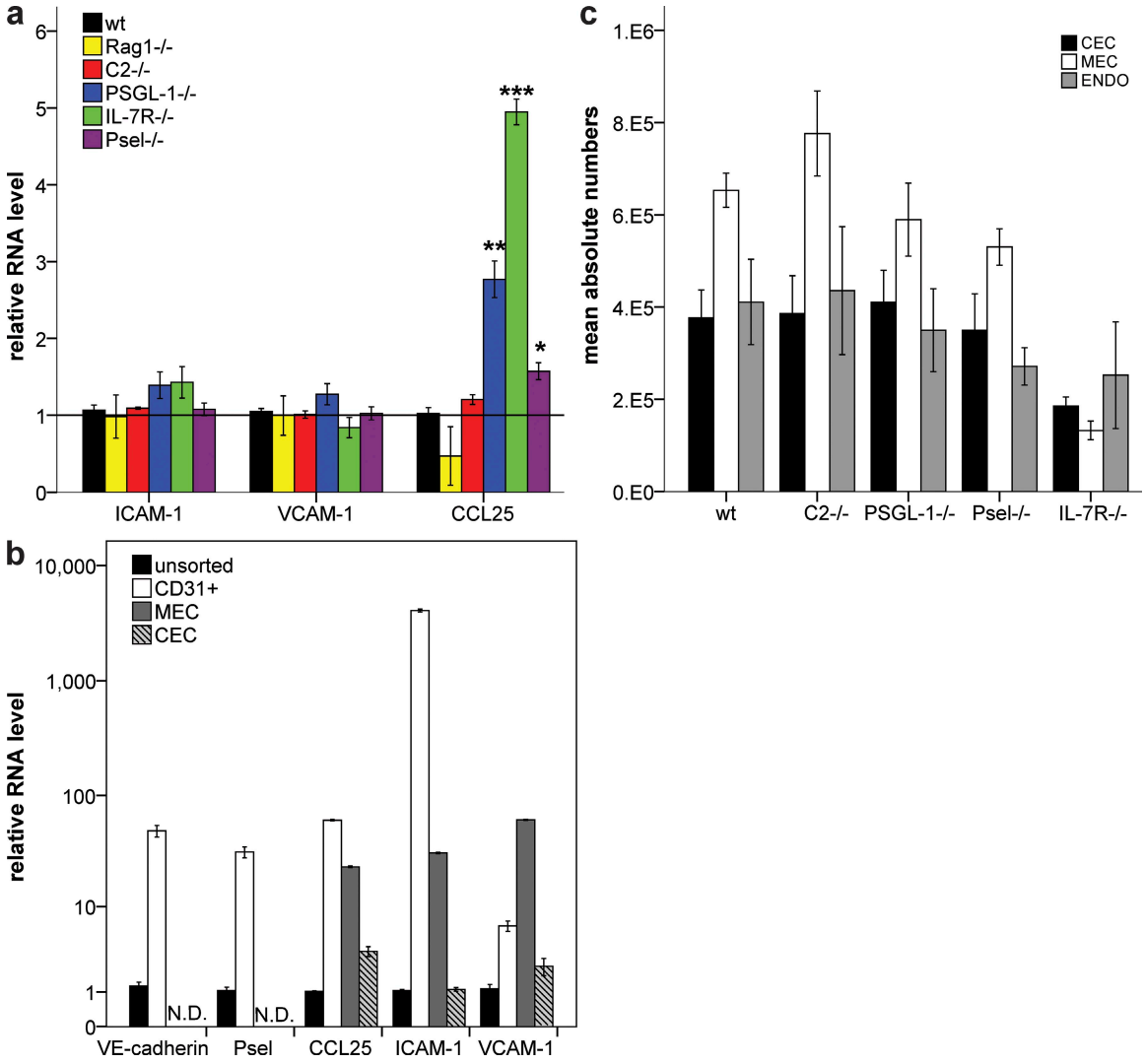

Figure 3. CCL25 RNA is expressed in thymic endothelial cells and is also highly expressed in hyperreceptive thymi of IL-7R$^{-/-}$ and PSGL-1$^{-/-}$ mice. (a) RNA levels of ICAM-1, VCAM-1, and CCL25 in the thymi of WT and RAG-$1^{-/-}$, C2GnT$1^{-/-}$, PSGL-$1^{-/-}$, IL-$7R^{-/-}$, and Psel$^{-/-}$ mice, as determined by qrtPCR. RNA levels were normalized to VE-cadherin and HPRT expression and expressed relative to WT (=1, as indicated). (b) Relative expression of the indicated genes in FACS-sorted WT thymic endothelial cells (ENDO; $CD45^{-}$, $CD31^{+}$, $CD144^{+}$), cortical epithelial cells (CEC; $CD45^{-}$, $Ly51^{hi}$, $G8.8^{+}$), and medullary epithelial cells (MEC; $CD45^{-}$, $Ly51^{int}$, $G8.8^{+}$) relative to expression in an unsorted sample. RNA levels were normalized to the reference genes HPRT and TbP. N.D., not detected. (c) Numbers of ENDO, CEC, and MEC in the thymi of the indicated mouse strains. For b and c, thymi were sequentially digested with collagenase and collagenase/dispase, and single-cell suspensions were analyzed by flow cytometry using reference beads to calculate absolute cell numbers. ENDO, CEC, and MEC were defined as in b. Data are representative of at least three independent experiments with at least five mice in a and c, and four mice in b (means ± SEM). Mice were sex matched and 35 ± 4 d old. C2, C2GnT1. *, $P < 0.05$; **, $P < 0.01$; and ***, $P < 0.001$.

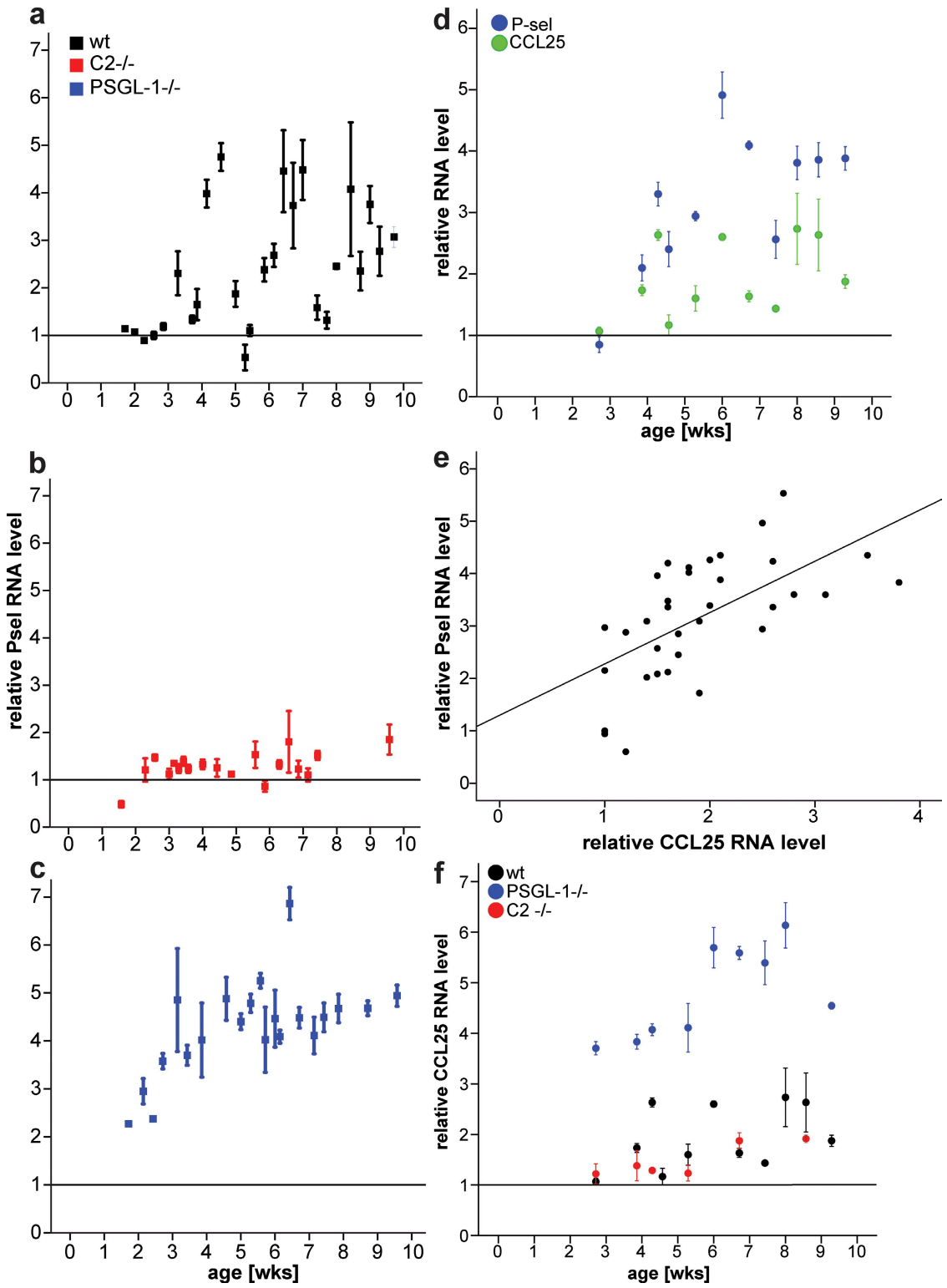

Figure 4. P-selectin and CCL25 RNA are periodically regulated in WT thymi. P-selectin RNA level as a function of time in (a) WT, (b) C2GnT1$^{-/-}$, or (c) PSGL-1$^{-/-}$ mice, as determined by qrtPCR, were normalized to VE-cadherin expression and expressed relative to WT values at 20 d of age (=1, as indicated). (d) Temporal expression of thymic P-selectin and CCL25 RNA as determined by qrtPCR using the reference genes VE-cadherin and HPRT in WT mice. (e) Scatter plot showing P-selectin expression as a function of CCL25 expression in the same samples used in d. The diagonal line shows linear regression. Thymic P-selectin expression and CCL25 RNA show a highly significant ($P < 0.001$) correlation (Pearson's $\rho = 0.607$). (f) Temporal thymic CCL25 RNA level as determined by qrtPCR normalized using the reference genes VE-cadherin and HPRT in WT, PSGL-1$^{-/-}$, and C2GnT1$^{-/-}$ mice. Expression levels

similar in WT and knockout thymi. To test whether differences in the occupation status of intrathymic niches could explain the observed differences in receptivity we intrathymically injected WT bone marrow cells into the thymi of the different knockout strains. We found significantly (three to five times) increased availability of intrathymic niche space in mice deficient for PSGL-1, P-selectin, or C2GnT1 (Fig. 5 d). Niche availability inversely correlated with thymic ETP content and was comparable in C2GnT1$^{-/-}$ and PSGL-1$^{-/-}$ thymi (Fig. 5, c and d), contrasting with the significant differences observed between these two mouse strains in short- and long-term receptivity, and pointing to additional mechanisms next to niche occupancy that are involved in the regulation of thymic TCP receptivity.

Thymic emigration of single-positive (SP) T cells is impaired in PSGL-1$^{-/-}$ mice

We next considered the possibility that mature thymocyte subsets or thymic T cell export rates might influence TCP receptivity. Thus, we examined whether T cell production in PSGL-1$^{-/-}$ and C2GnT1$^{-/-}$ mice was different from WT mice. Cell-surface marker analysis of maturing thymocyte subsets showed increased frequencies of semimature (CD24^{+}, CD69^{+}, CD62L^{lo}, Qa-2^{-}) and mature (CD24^{lo}, CD69^{-}, Lsel^{hi}, Qa-2^{+}) (10–12) CD4^{+} and CD8^{+} thymocytes in PSGL-1$^{-/-}$ thymi (Fig. 6 a) but not in C2GnT1$^{-/-}$ thymi when compared with WT controls. qrtPCR analysis of FACS-sorted mature (CD44^{lo}, CD62L^{hi}, Qa-2^{+}) CD8^{+} and CD4^{+} thymocytes revealed a significant increase in RNA levels of T cell maturation markers (sphingosine-1-phosphate [S1P]–lyase, the transcription factor KLF2, and its target S1P$_1$; Fig. S4, a–c), confirming a high maturation status of accumulated SP thymocytes in PSGL-1$^{-/-}$ thymi, suggesting impaired thymic emigration in these mice.

We used intrathymic FITC injections as well as quantization of T cell receptor excision circles (TRECs) to measure thymic exit rates and found, consistent with these observations, that mature PSGL-1$^{-/-}$ T cells leave the thymus at a significantly lower rate than WT T cells, whereas C2GnT1$^{-/-}$ T cells emigrated at a rate comparable to WT T cells (Fig. 6, b and c).

The reduced thymic output in PSGL-1$^{-/-}$ mice was furthermore associated with decreased T cells in the periphery. In PSGL-1$^{-/-}$ mice, we found significantly reduced numbers of CD4 and CD8 cells in peripheral blood, whereas T cell numbers in C2GnT1$^{-/-}$ mice were comparable to WT controls (Fig. 6 d). Reduced thymic T cell output together with reduced numbers of peripheral T cells in PSGL-1$^{-/-}$ mice led us to hypothesize that thymic T cell output and/or the size of the peripheral lymphocyte pool might modulate thymic P-selectin expression and, thus, TCP receptivity.

Peripheral lymphocyte levels affect thymic TCP receptivity

To test for the potential effect of peripheral T cell lymphopenia on thymic P-selectin expression, we compensated the reduced peripheral T cell numbers in PSGL-1$^{-/-}$ mice by transfer of 20 × 10^6 WT lymphocytes. 2 d after lymphocyte transfer, thymic P-selectin expression and receptivity for TCPs was reduced by 50–60% when compared with saline-injected controls (Fig. 7, a and b; and Fig. S5 a).

These observations suggested that depletion of peripheral T cells might lead to increased P-selectin expression and, thus, increased thymic progenitor receptivity. To test this hypothesis, we depleted peripheral CD4 and CD8 T cells in WT mice with anti-CD4 and -CD8 antibodies, whereas thymic T cell numbers remained unchanged (Fig. S5 b). Both thymic P-selectin RNA and TCP receptivity increased nearly threefold within 24 h after T cell depletion when compared with saline-treated controls (Fig. 7, c and d). Collectively, these data support the hypothesis that thymic TCP importation can be altered by changes in peripheral lymphocyte levels.

Thymic P-selectin expression correlates with plasma S1P levels

Aside from its role in lymphocyte egress from lymphoid organs, S1P is involved in the regulation of endothelial barrier function and the expression of endothelial adhesion molecules, including P-selectin (13–16), making this lipid metabolite a potential candidate to affect thymic endothelial P-selectin expression.

To test whether S1P levels vary under physiological conditions, we used liquid chromatography–mass spectrometry/mass spectrometry (LC-MS/MS) to determine S1P levels in the plasma of WT and the previously mentioned mouse strains. We found that IL-7R$^{-/-}$ and RAG-1$^{-/-}$ mice had S1P plasma levels comparable to WT controls. S1P was moderately reduced in PSGL-1$^{-/-}$ mice (23%; $P = 0.044$) and slightly but not significantly reduced in C2GnT1$^{-/-}$ mice (10%; $P = 0.349$) when compared with WT controls. In contrast, Psel$^{-/-}$ mice had increased S1P plasma levels (26%; $P = 0.033$) compared with WT (Fig. 8 a).

Given that thymic P-selectin expression is periodically expressed in WT thymi, we tested whether plasma S1P levels were also changing periodically and, if so, whether S1P levels correlated with thymic P-selectin RNA. S1P plasma levels varied in 19–65-d-old WT mice within a range of 2–3.7 μM. Changes in plasma S1P concentration correlated positively and significantly ($P < 0.001$) with changes in thymic P-selectin RNA (Fig. 8, b and c), suggesting that S1P plasma level and thymic P-selectin expression are linked.

S1P agonist FTY720 reduces thymic P-selectin expression

S1P has been shown to induce RNA expression of VCAM-1 and E-selectin in human endothelial cells mediated by NF-κB (13).

are expressed relative to the corresponding value found in WT thymi at 20 d of age (=1, as indicated). Data in a–c show a combination of three out of a total of five independent experiments; data in d and f are representative of at least five independent experiments (means ± SEM). For all time-course experiments, at least four mice per time point were used. Only female mice were used in time-course experiments. C2, C2GnT1.

Because both mouse E- and P-selectin promotor regions share transcription factor binding sites, including those for NF-κB and activating transcription factor (ATF) (17), S1P receptor (S1PR) signaling could potentially also modulate P-selectin expression. One hallmark of S1PR signaling is its concentration dependency; superphysiological levels of S1P often inhibit the very same processes that are activated under lower concentrations (18). S1P treatment of the mouse endothelial cell line bend.3 showed that S1P can directly modulate P-selectin expression in endothelial cells (Fig. 9 a). Concentrations up to 1 μM S1P had a significant positive effect on P-selectin RNA expression when compared with control cells, whereas a superphysiological concentration of S1P (10 μM) significantly reduced P-selectin expression below control values. To determine whether an increased S1P level also decreases P-selectin expression on thymic endothelium in vivo, we treated IL-7R$^{-/-}$ mice, which have a normal level of plasma S1P (Fig. 8 a) and only few T and B cells, for 3 d with the S1P analogue FTY720 (19). Treatment of IL-7R$^{-/-}$ mice with FTY720 significantly reduced thymic P-selectin RNA expression (Fig. 9 b). Treatment of WT mice with FTY720 also resulted in a reduction of thymic P-selectin expression and was associated with reduced thymic TCP receptivity (Fig. 9, c and d), suggesting that S1PR signaling is involved in the regulation of thymic P-selectin expression and, thus, thymic TCP receptivity. Furthermore, mice treated for 3 d with FTY720 had significantly ($P = 0.002$) reduced DN1 thymocyte numbers compared with controls (Fig. S6, a and b). Collectively, this set of data shows that FTY720 treatment reduces thymic TCP entry.

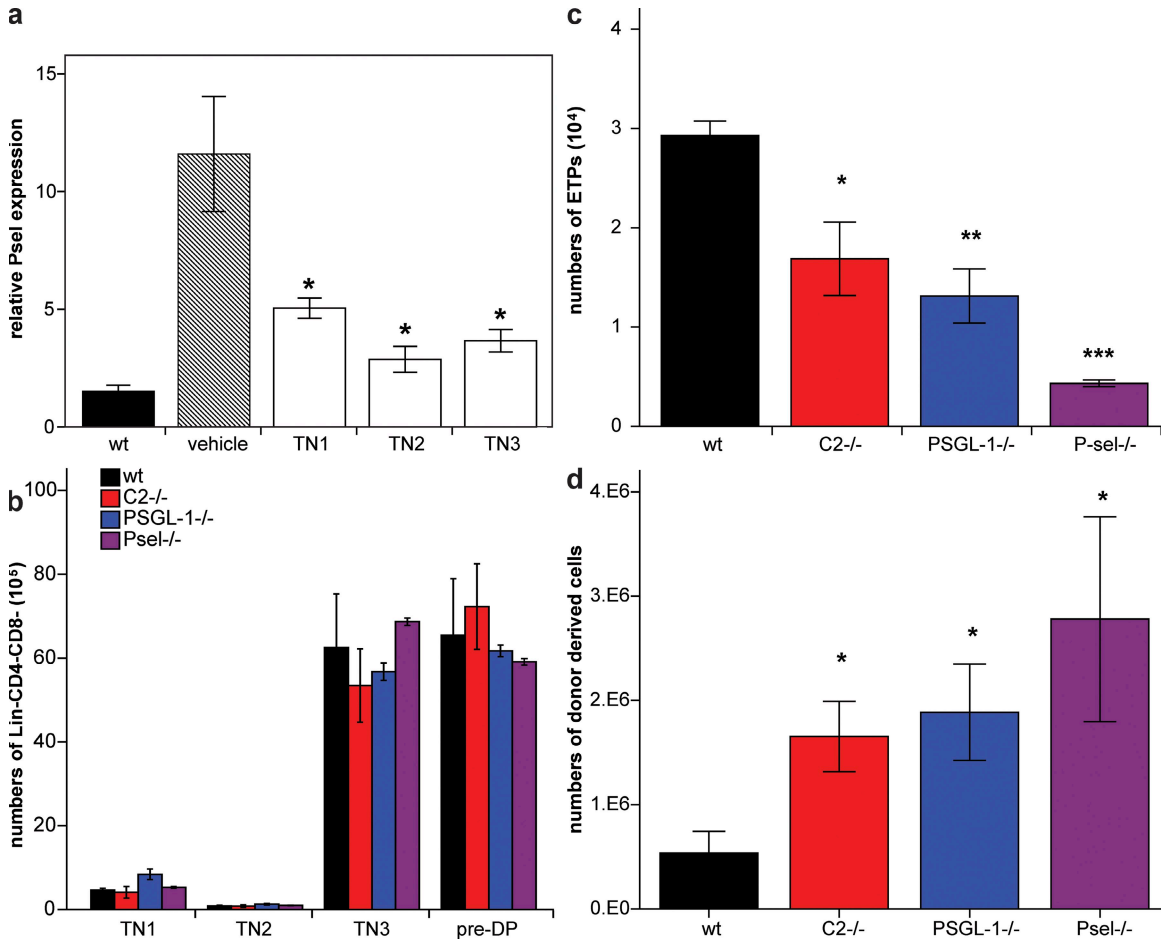

Figure 5. The niche occupancy model does not explain differences in thymic TCP receptivity between C2GnT1$^{-/-}$ and PSGL-1$^{-/-}$ mice. (a) TN1–3 thymocyte subsets were purified by FACS and i.v. injected into nonirradiated IL-7R$^{-/-}$ mice. The figure shows the thymic P-selectin RNA level as determined by qrtPCR using the reference gene VE-cadherin 12 d after injection. P-selectin levels are expressed relative to sex- and age-matched WT mice (=1, as indicated). *, $P < 0.05$, significantly reduced P-selectin expression relative to vehicle-injected control. (b) Numbers of TN thymocyte subsets are similar in the thymi of WT and C2GnT1$^{-/-}$, PSGL-1$^{-/-}$, and Psel$^{-/-}$ mice. TN cells were defined as Lin^{lo}, CD4^{-}, CD8^{-}, with TN1 (CD25^{-}CD44^{+}), TN2 (CD25^{+}CD44^{+}), TN3 (CD25^{+}CD44^{-}), and pre-DP (CD25^{-}CD44^{-}). (c) Numbers of ETPs (Lin^{lo}, CD44^{+}, CD25^{-}, cKit^{hi} Sca-1^{+}) are significantly reduced in C2GnT1$^{-/-}$, PSGL-1$^{-/-}$, and P-selectin–deficient mice when compared with WT mice. (d) Numbers of donor-derived cells 14 d after intrathymic injection of WT bone marrow cells are increased in C2GnT1$^{-/-}$, PSGL-1$^{-/-}$, and Psel$^{-/-}$ mice compared with WT controls. Data are representative of three independent experiments with at least four mice used in a, and at least seven mice used in b–d (means ± SEM). Mice were sex matched and 45 ± 4 d old in a, and 35 ± 4 d old in b–d. C2, C2GnT1. *, $P < 0.05$; **, $P < 0.01$; and ***, $P < 0.001$.

To examine whether local tissue S1P gradients or overall plasma S1P levels modulate P-selectin expression, we treated mice with 2-deoxypyridoxine (DOP) to inhibit the S1P-degrading enzyme S1P-lyase, thereby increasing S1P levels in lymphoid tissues but not in blood, disrupting the S1P gradient between lymphoid tissues and blood or lymph (20). Administration of DOP resulted in a significant reduction of thymic P-selectin RNA and TCP receptivity, suggesting that disruption of the S1P gradient associated with a local increase of S1P in lymphoid tissues leads to down-regulation of thymic P-selectin and TCP receptivity (Fig. 9, e and f; and Fig. S7).

Finally, we analyzed whether changes in P-selectin expression after lymphocyte boost and depletion were associated with corresponding changes in plasma S1P levels. 48 h after depletion of CD4 and CD8 T cells, S1P levels were increased by 34% when compared with saline-injected controls ($P = 0.052$; Fig. 10 a). Boosting PSGL-$1^{-/-}$ mice with T cells, B cells, or a 1:1 mixture of T and B cells was associated with a reduction in plasma S1P levels 3 d after cell transfer. B cells reduced S1P levels by 40%, T cells reduced S1P levels by 34%, and the T and B cell mixture reduced S1P levels by 47% (Fig. 10 b). Collectively, this set of data shows that short-term perturbation of peripheral lymphocyte numbers can induce changes in plasma S1P levels that in turn might be linked to control of thymic P-selectin expression.

DISCUSSION

P-selectin and CCL25 are known to facilitate TCP entry into the thymus, and thymic P-selectin expression has been shown to correlate with thymic TCP receptivity (2–4, 21). In this study, we extend the knowledge about the regulation of TCP entry into the thymus and provide evidence that P-selectin and CCL25 themselves are regulated in a temporal and quantitative manner. Most TCPs described so far express functional

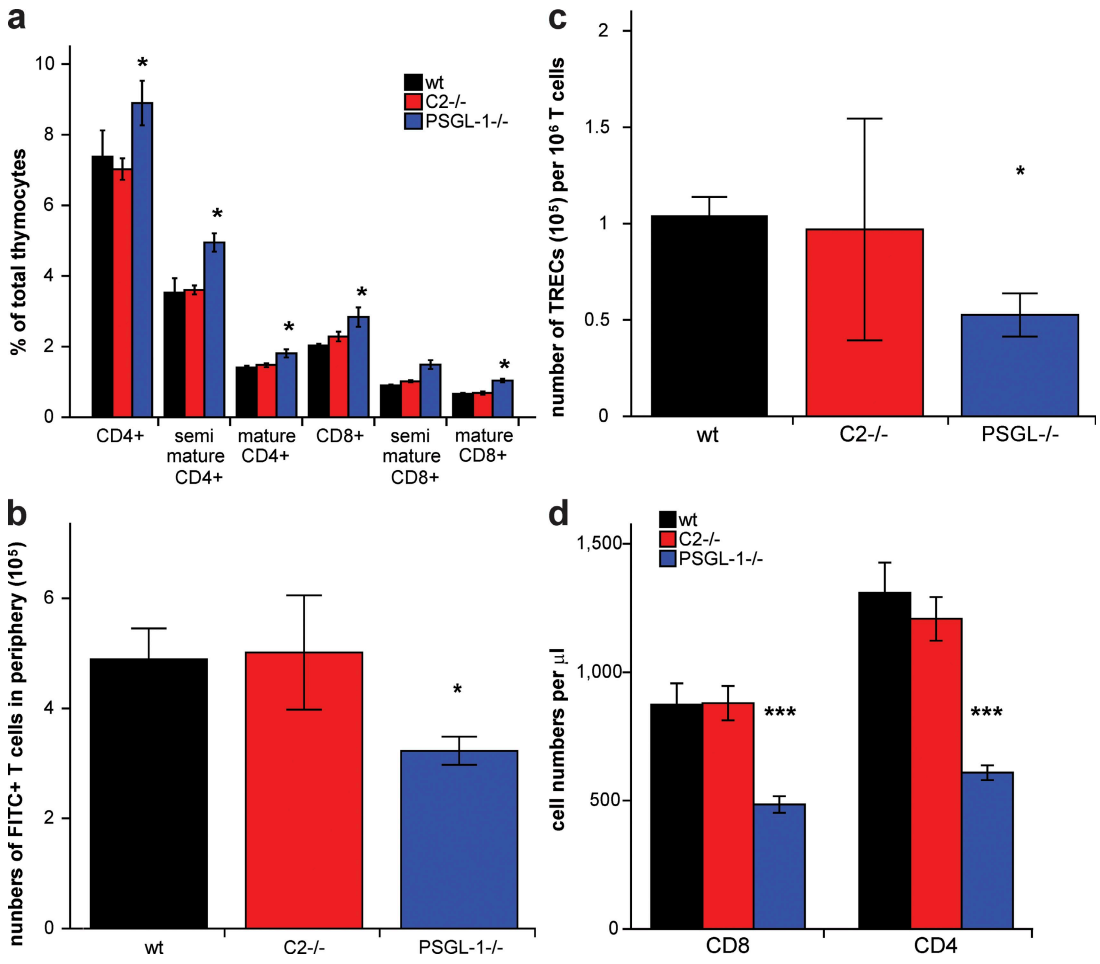

Figure 6. PSGL-1 deficiency is associated with reduced thymic T cell output and peripheral T cell lymphopenia. (a) Flow cytometry analysis of CD4 and CD8 SP thymocytes, and semimature ($CD24^+$, $CD69^+$, $Qa\text{-}2^-$, $LseI^{lo}$) and mature ($CD24^{lo}$, $CD69^-$, $Qa\text{-}2^+$, $LseI^{hi}$) $CD4^+$ and $CD8^+$ thymocyte subsets in WT, C2GnT1$^{-/-}$, and PSGL-1$^{-/-}$ mice. (b) Total numbers of $FITC^+$, $LseI^{hi}$, $CD4^+$ and $FITC^+$, $LseI^{hi}$, $CD8^+$ T cells in lymph nodes and spleen of WT, C2GnT1$^{-/-}$ and PSGL-1$^{-/-}$ mice 36 h after intrathymic FITC injection. (c) Numbers of TRECs per 10^6 spleen-derived T cells in WT, C2GnT1$^{-/-}$, and PSGL-1$^{-/-}$ mice as measured by qrtPCR. (d) Numbers of $CD4^+$ or $CD8^+$ cells per microliter of peripheral blood in age-matched WT, C2GnT1$^{-/-}$, and PSGL-1$^{-/-}$ mice. Data are representative of three (a, b, and d) and two (c) independent experiments, with at least four mice per group in a–c and three mice per group in d (means ± SEM). Mice were sex matched and 36 ± 4 d old. C2, C2GnT1. *, $P < 0.05$; and ***, $P < 0.001$.

P-selectin ligands (7); regulation of thymic P-selectin expression thus offers an effective way to control TCP importation on a general level but does not provide specificity to the thymic recruitment process. Chemokines are likely to provide specificity, and several studies have highlighted the role of CCL25 in TCP recruitment (4, 22, 23). We show that thymic endothelial cells as well as epithelial cells produce CCL25 RNA, and that thymic CCL25 is expressed periodically in parallel with P-selectin. Hence, high expression of CCL25 should preferentially enhance the thymic homing of TCPs expressing high levels of CCR9. Such CCR9^{hi} TCPs have been shown to be more efficient in producing T cells than their CCR9^{lo} counterparts (22). The elevated levels of CCL25 RNA in the thymi of PSGL-1$^{-/-}$ mice are thus likely the explanation for the higher receptivity we observe in PSGL-1$^{-/-}$ mice at time points when they express similar amounts of P-selectin as WT thymi. Increased expression of CCL25 in the thymi of IL-7R$^{-/-}$ and PSGL-1$^{-/-}$ mice likely also explains the relatively high importation of Lin^{-}CFSE^{+} cells in the short-term homing assays.

Although the presence of homing molecules like P-selectin and CCL25 is important in regulating the quantity and quality of TCPs entering the thymus, deficiencies in these proteins can be compensated by functional redundancy among the homing molecules and by intrathymic compensatory mechanisms (24). We show that although PSGL-1$^{-/-}$, C2GnT1$^{-/-}$, and Psel$^{-/-}$ mice have reduced ETP numbers, they have normal thymic cellularity, indicating that increased intrathymic proliferation can compensate for a lack in ETP numbers. Whether the T cells that result from compensatory proliferation of a reduced ETP pool are qualitatively identical to T cells that resulted from a large ETP pool remains to be investigated.

The temporal expression of thymic P-selectin we observed is remarkably stable for the first 3 wk after birth and

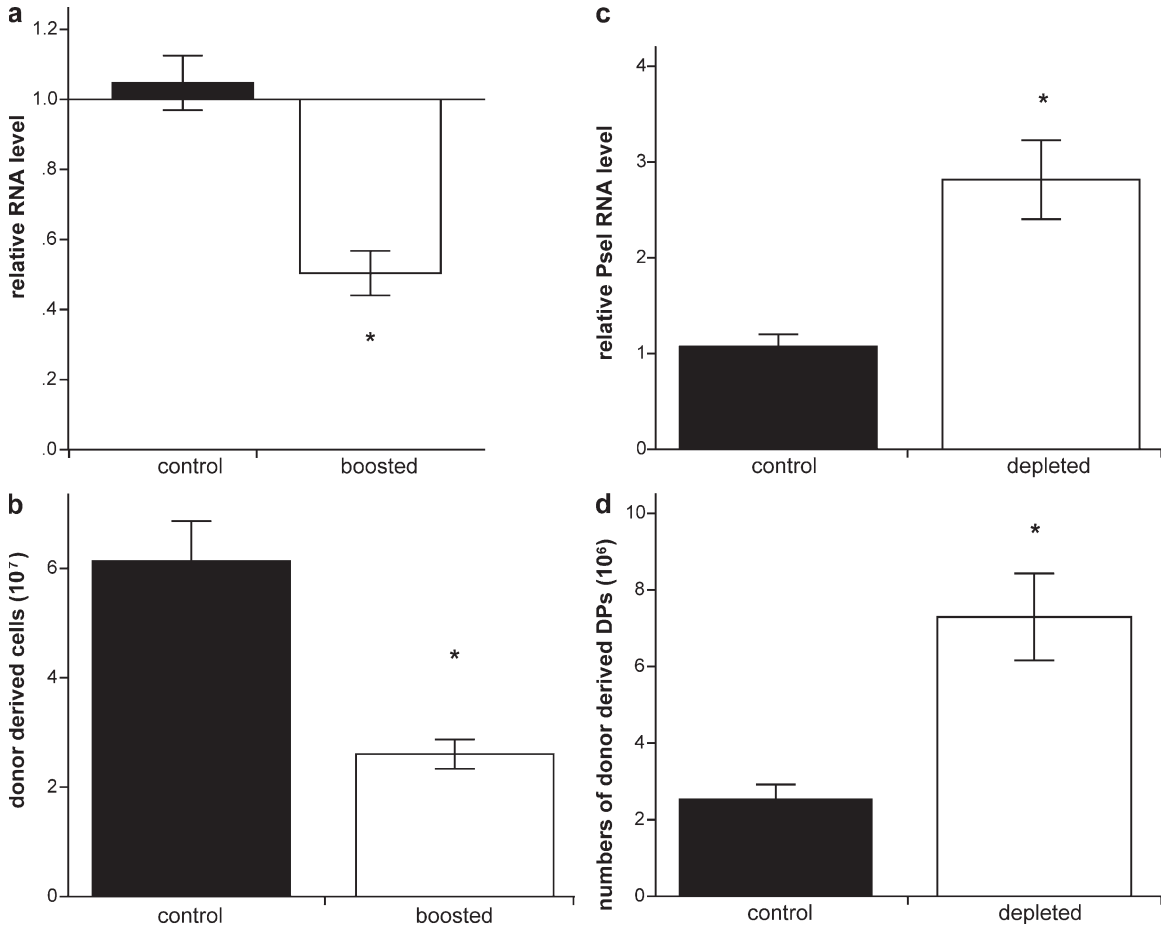

Figure 7. Size of the peripheral lymphocyte pool modulates thymic P-selectin expression and thymic receptivity. (a) Thymic P-selectin RNA levels in PSGL-1$^{-/-}$ mice were determined 2 d after i.v. transfer of 20 × 10^6 WT lymphocytes (boosted) or vehicle alone (control). (b) Numbers of donor-derived DP thymocytes were determined by flow cytometry 3 wk after transfer of WT bone marrow into vehicle (control) or lymphocyte-injected (boosted) PSGL-1$^{-/-}$ mice. (c) Thymic P-selectin RNA levels in WT mice 24 h after i.p. injection of anti-CD4/CD8 antibodies (depleted) or vehicle alone (control). (d) Numbers of donor-derived DP thymocytes were determined by flow cytometry 3 wk after bone marrow transfer into CD4/CD8 T cell–depleted (depleted) or control WT mice. Bone marrow transfers were performed on day 2 after boost or depletion. Data are representative of two independent experiments with at least six mice (means ± SEM). Mice were sex-matched and 42 ± 4 d old. RNA levels were normalized to VE-cadherin expression and expressed relative to values from vehicle-treated controls (=1, as indicated). *, $P < 0.05$.

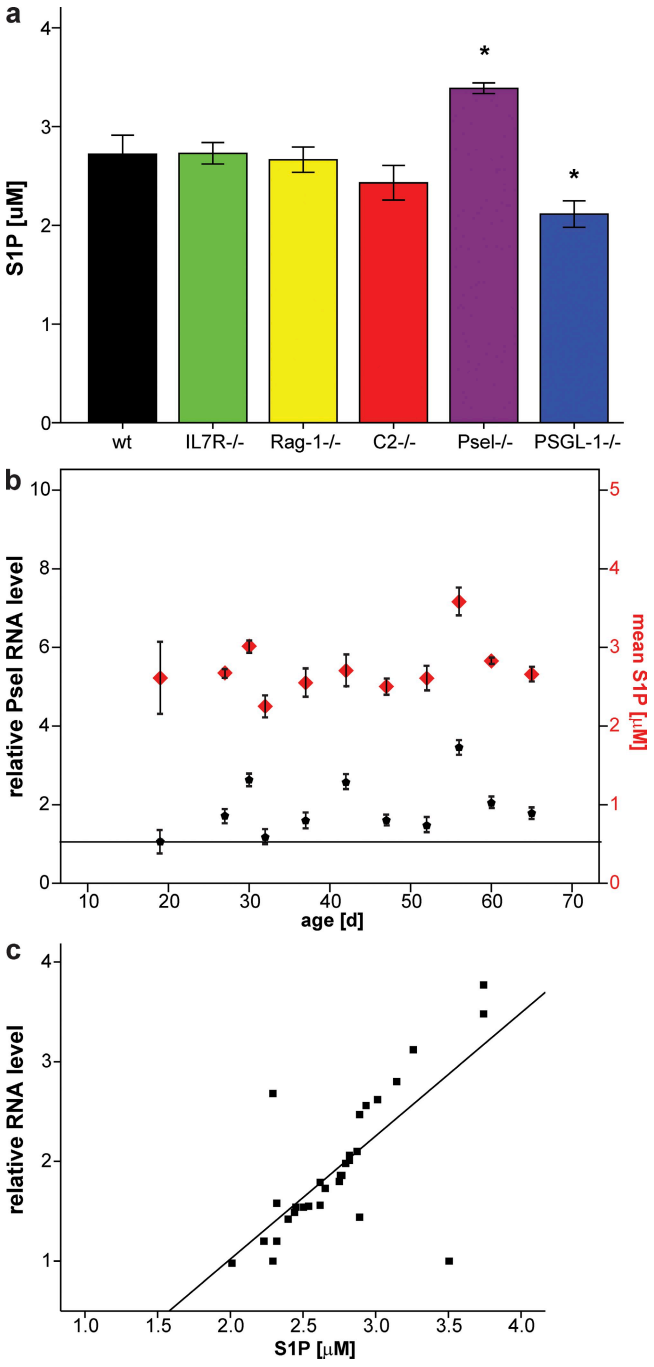

Figure 8. Plasma S1P correlates with thymic P-selectin RNA expression over time in WT mice. (a) Plasma concentration of S1P in the indicated mouse strains as determined by LC-MS/MS. (b) Mean plasma S1P concentration (red) and relative mean thymic P-selectin expression (black) in 19–65-d-old WT mice. (c) Scatter plot showing P-selectin expression from b as a function of S1P plasma concentration (μM). The diagonal line shows linear regression. S1P plasma concentration and thymic P-selectin RNA show a highly significant ($P < 0.001$) correlation (Pearson's $\rho = 0.735$). Data in a are representative of three independent experiments with at least five sex-matched mice that were 34 ± 4 d old, and data in b and c are representative of two independent experiments with at least three mice per time point (means ± SEM). RNA levels were normalized to VE-cadherin expression and were expressed relative to values at day 19 (=1, as indicated). Only female mice were used for time-course experiments. C2, C2GnT1. *, $P < 0.05$.

starts to oscillate around the time of weaning. The increase in P-selectin and CCL25 expression coincides with the second wave of postnatal TCPs that seed the thymus around days 18–22 after birth (25), a period when the neonatal immune system is highly active and develops full independence of the maternal immune system (26). P-selectin was expressed with a periodicity of 2 wk, in agreement with an earlier study that found a 2-wk wave-like pattern of filling, occupation, and emptying of intrathymic niches (8). However, another study showed a periodicity for thymic receptivity of about 3–4 wk (2). This discrepancy could be caused by the use of nonsynchronized mice in our work, whereas the earlier study used irradiation or intrathymic injection of bone marrow cells to synchronize the thymi of recipient mice.

One underlying cause of the periodic expression of thymic P-selectin expression could be endothelial cell turnover. However, based on the longevity of endothelial cells, which is estimated to be in the range of months to years, it is unlikely that cell turnover causes the cyclical P-selectin expression we observed (27). It is also unlikely that fluctuations in CCL25 expression are caused by a highly proliferative subset of medullary epithelial cells (28), as we also observed CCL25 in cortical epithelial and, particularly, in endothelial cells that produce the bulk of thymic CCL25 RNA. Instead, our observations point to the occupation status of ETP niches as a regulator for the periodicity of homing molecule expression and thymic receptivity. We found that mice with permanently contracted ETP pools lacked the periodicity of P-selectin or CCL25, supporting a model whereby ETP numbers regulate the periodic expression of P-selectin and CCL25 via a negative feedback signal. In this model, full ETP niches would trigger a negative feedback to close the thymic gates and keep them closed for 2 wk, which is the time required for TCPs to reach the TN3 developmental stage (12, 24). ETPs reside anatomically close to their thymic entry sites in the perimedullary cortical regions and asynchronously migrate from there deeper into the cortex (12). Given that the steady egress of cells from the ETP sites occurs at a constant rate, the shrinking ETP pool size could indeed function as a timer to prepare the TCP entry sites to up-regulate recruitment molecules, enabling the next wave of TCPs to enter the thymus. Thus, in mice that lack functional P-selectin–PSGL-1 interaction, TCP entry is impaired and occurs at a constant rate. Hence, ETP numbers in these mice do not change over time, leaving P-selectin and CCL25 levels relatively stable.

Although periodicity of thymic receptivity seems to be exclusively regulated by an internal negative feedback signal triggered by ETP numbers, we found that the amount of homing molecules expressed on the thymic endothelium is dynamically regulated by internal and external feedback signals. The occupation status of intrathymic niches supporting

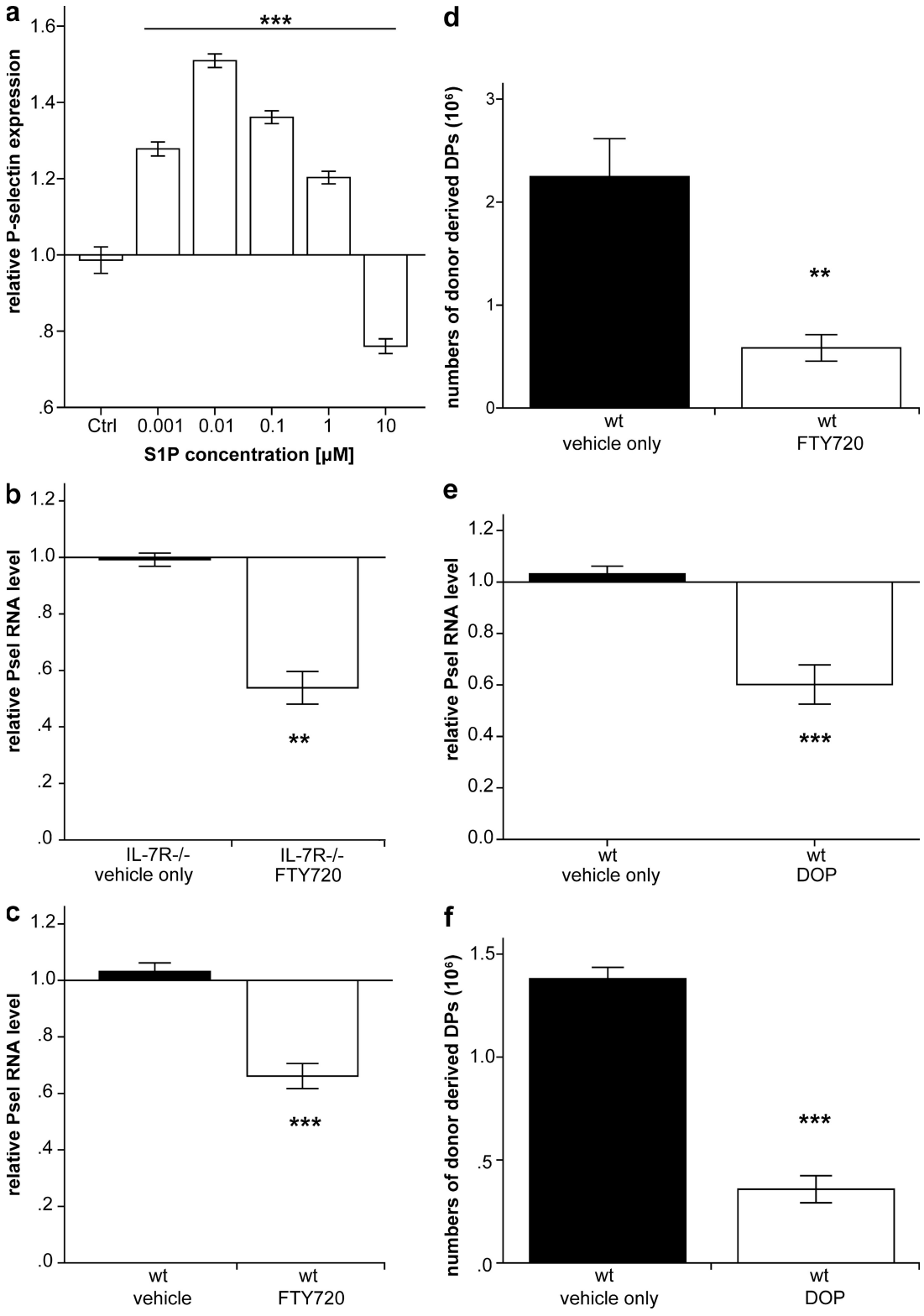

Figure 9. The immunomodulating drugs FTY720 and DOP alter endothelial P-selectin expression and thymic receptivity. (a) S1P dose–response on P-selectin RNA expression in bend.3 cells that were cultured in the indicated concentrations of S1P for 12 h. Control wells received media only ($n = 8$). (b and c) Thymic P-selectin RNA levels were assessed by qrtPCR and normalized to the reference gene VE-cadherin in (b) IL-7R$^{-/-}$ and (c) WT mice i.p. injected with 1 mg/kg FTY720 or vehicle alone on three consecutive days. (d) Numbers of donor-derived DP thymocytes 3 wk after bone marrow transfer into WT recipients that were treated for 3 d with FTY720 or vehicle alone. (e) Thymic P-selectin RNA levels in WT mice after treatment with

DN3 thymocytes has been proposed previously as a mechanism that could limit entry of new TCPs (6). Although reconstitution of IL-7R$^{-/-}$ mice with TN3 cells was in agreement with such a mechanism, we found that C2GnT1$^{-/-}$ and PSGL-1$^{-/-}$ mice had the same DN thymocyte subset distribution and intrathymic niche availability but differed greatly in thymic TCP importation. This observation pointed to the existence of an additional mechanism, other than intrathymic niche occupancy, that regulates thymic Psel/CCL25 expression and receptivity. Manipulation of the peripheral lymphocyte pool led, within a relatively short period of time, to significant changes in the intensity of thymic TCP importation, providing evidence for a rapid feedback mechanism between the peripheral lymphocyte pool and thymic TCP recruitment. Such a mechanism is absent in RAG-1$^{-/-}$ mice that are lymphopenic but have thymi that are very low in P-selectin/CCL25 and TCP receptivity. Fundamental disturbances in thymic architecture noted previously in RAG-1$^{-/-}$ mice may preclude formation of proper negative feedback mechanism (6, 29). Although the peripheral lymphocyte pool is able to alter the intensity of thymic TCP receptivity, our data do not indicate that it also affects the periodicity of P-selectin/CCL25 expression. Furthermore, homeostatic mechanisms maintain steady lymphocyte numbers over time (30), making it unlikely that the peripheral lymphocyte pool contributes to periodicity in thymic TCP importation.

Our analyses have uncovered two novel phenotypes associated with PSGL-1 deficiency, T cell lymphopenia, and a reduced exit rate of T cells from the thymus. We have shown previously that PSGL-1$^{-/-}$ T cells have ~10% reduced homing to the spleen (31); although this reduced homing capacity may marginally skew determination of the thymic exit rate of PSGL-1$^{-/-}$ T cells, it is unlikely to translate in the 50% reduced exit rate we have determined for these cells.

We identified S1P as a potential mediator translating changes in the peripheral lymphocyte pool into altered thymic TCP receptivity. The phospholipid S1P is known to activate the NF-κB pathway through the $S1P_3$ receptor (32) and to induce transcription of cytokines, chemokines, and adhesion molecules, including P-selectin (17, 33). Using the mouse endothelial cell line bend.3, we showed that S1P has an opposing dose-dependent effect on P-selectin expression, in agreement with a previous study performed on human cells (16), suggesting that S1P might act directly on endothelial cells and that the effects we observed in vivo are not caused by indirect effects. The observation that DOP treatment also inhibits thymic TCP receptivity suggests that local S1P gradients modulate TCP importation. Furthermore, our findings expand the known pharmacological activities of DOP and FTY720, but the physiological consequences of prolonged drug treatment remain to be investigated.

The finding that boosting or depleting peripheral lymphocyte numbers correlated with rapid changes in plasma S1P levels suggests that peripheral lymphocytes and S1P metabolism interact. However, it remains to be determined whether lymphoyctes directly or indirectly modulate S1P level. Our data also show that S1P levels in lymphopenic IL-7R$^{-/-}$ and RAG-1$^{-/-}$ mice were not increased compared with WT mice, which seems to contradict the data from the boost/depletion experiments. We favor the explanation that compensatory mechanisms described previously (34–36) might lead to normal S1P levels in those mice. P-selectin or PSGL-1 deficiency is associated with altered blood S1P levels, indicating that the presence of these molecules is important in S1P homeostasis. It has been shown that P-selectin–deficient mice have an increased level of plasma high-density lipoprotein (HDL) (37). Because HDL binds free S1P, thereby protecting it from degradation (38), the increased S1P level we observe in Psel$^{-/-}$ mice could be explained by increased plasma HDL. Furthermore, the phenotype of PSGL-1$^{-/-}$ mice is to some degree reminiscent of the phenotype of sphingosine-kinase–deficient mice (35) in that both knockout strains have reduced S1P plasma levels and a corresponding increased $S1P_1$ expression on T cells, reduced thymic output, and reduced numbers of circulating T cells, whereas T cells in lymph nodes and spleens are normal. Collectively, these findings suggest a possible interaction between S1P metabolism and the P-selectin–PSGL-1 axis. However, the exact nature of this mechanism needs to be further investigated.

Boost/depletion experiments revealed a surprisingly rapid feedback mechanism in the regulation of thymic TCP entry. We hypothesize that boosting or depleting the peripheral T cell pool leads to increased cell stress that in turn could trigger an acute reaction leading to altered S1P level. In support of this hypothesis are the findings that S1P levels change under stress situation and inflammation (39–41). Furthermore, the observation that hematopoietic stem and progenitor cells also respond to S1P gradients (42, 43) suggests a potential bifunctional role of S1P in modulating thymic TCP receptivity by altering adhesion molecule expression on the thymic endothelium and by modulating the migration pattern of hematopoietic stem and progenitor cells, including TCPs.

How can lymphocytes, which are only marginally involved in S1P production or degradation (18, 44), induce short-term changes in S1P levels? There is clear evidence that erythrocytes are one major source for plasma S1P, and although genetic evidence is still lacking, there are strong indications that

30 mg/liter DOP in the drinking water for 3 d. (f) Numbers of donor-derived DP thymocytes as determined by flow cytometry 3 wk after bone marrow transfer into WT mice treated for 3 d with 30 mg/ml DOP in the drinking water or with vehicle alone before the bone marrow transfer. Data are representative of at least three independent experiments with at least five mice (means ± SEM). Mice were 33 ± 5 d old and sex matched. RNA levels were normalized to VE-cadherin expression and expressed relative to values from vehicle-treated controls (=1, as indicated). Bone marrow transfers were done 1 d after FTY720 or DOP treatments were stopped. **, $P < 0.01$; and ***, $P < 0.001$.

endothelial cells are also involved in S1P homeostasis by removing S1P from circulation and/or releasing it into circulation (18, 34–36, 45). Although they do not produce S1P, platelets have been shown to store and release large amounts of S1P (46) and may thus contribute to S1P homeostasis. We hypothesize that lymphocytes indirectly modulate S1P production or degradation by cytokine release or by direct interaction with cells that control S1P homeostasis. Interaction of peripheral lymphocytes with thymic endothelial cell–expressed P-selectin and, thus, a direct signaling through thymic P-selectin can, however, be excluded as a possible feedback mechanism, as resting peripheral lymphocytes do not express functional P-selectin ligand (47).

Based on our data, we propose a model in which thymic Psel/CCL25 expression and, consequently, thymic TCP receptivity are controlled by two feedback mechanisms. The first mechanism active under homeostatic conditions triggers a feedback signal from the thymic perivascular region, depending on the quantity and possibly also the quality of immigrated ETPs. This intrathymic signal regulates the periodicity of thymic P-selectin and CCL25 expression. Mouse strains with reduced ETP numbers, such as IL-7R$^{-/-}$, RAG-1$^{-/-}$, PSGL-1$^{-/-}$, and C2GnT1$^{-/-}$ mice, have no periodic expression in thymic P-selectin and CCL25. The second mechanism triggers a feedback signal depending on the size of the peripheral lymphocyte pool and is active especially under acute conditions affecting the intensity of Psel/CCL25 expression. The thymic vascular gates thus integrate both feedback signals and control the entry of new TCPs into the thymus by adjusting the amount and periodicity of expression of recruitment molecules on thymic endothelial cells. These results provide new insights into the mechanisms that regulate periodic TCP importation into the thymus and demonstrate that the thymus responds to internal and external cues to regulate T cell formation.

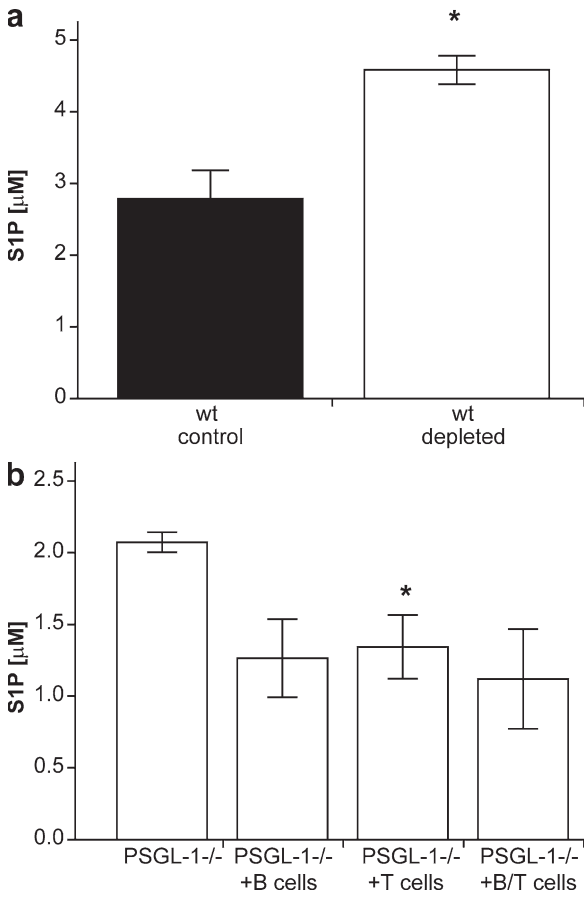

Figure 10. Plasma S1P levels are modulated by the size of the peripheral lymphocyte pool. (a) S1P level in plasma of WT mice 2 d after in vivo depletion of CD4 and CD8 T cells by i.p. injection of depleting antibodies measured by LC-MS/MS. Control mice received saline only. (b) Plasma S1P level in PSGL-1–deficient mice 2 d after adoptive transfer of WT B cells, T cells, or a 1:1 mix of T and B cells determined by LC-MS/MS. Data are representative of two independent experiments with at least four mice (means ± SEM). Mice were sex matched and 42 ± 2 d old. *, $P < 0.05$.

MATERIALS AND METHODS

Mice. C57BL/6 (CD45.2), congenic C57BL/6 (CD45.1), PSGL-1$^{-/-}$ (B6.Cg-Selplg^{tm1Fur}), Psel$^{-/-}$, IL7R$^{-/-}$, and RAG-1$^{-/-}$ mice, all backcrossed onto a C57BL/6 background, were purchased from the Jackson Laboratory. C2GnT1$^{-/-}$ mice were backcrossed onto C57BL/6 mice for at least eight generations (obtained from J. Marth, Howard Hughes Medical Institute, University of California, San Diego, La Jolla, CA) (5), and were maintained and bred at the specific pathogen-free animal facility at the Biomedical Research Centre. For time-course experiments, only female mice were used. All animal experiments were performed according to institutional guidelines and were approved by the Animal Care Committee of the University of British Columbia.

Tissue extraction. Mice were sacrificed and perfused with PBS, 5 mM EDTA. Single-cell suspensions of peripheral lymph nodes and spleens were prepared by squeezing tissues through a mesh. Thymic cell suspensions were obtained by gently squeezing the thymus between two frosted glass slides and washing it several times with RPMI 1640, 2% FCS, 2 mM EDTA. The thymocyte-containing suspension fraction was filtered and kept for flow cytometry analysis. The remaining nonsuspension fraction was either directly processed for qrtPCR or flow cytometry analysis, or stored at −80°C.

Flow cytometry and cell sorting. Cell suspensions were stained in staining buffer (PBS, 2% FCS, 2 mM EDTA) with titrated amounts of the antibodies specified (Table S1). Samples were analyzed on a flow cytometer (FACSCalibur or LSRII; BD), and cell sorting was performed on a FACSVantage or FACSAria (BD). Data were analyzed with FlowJo software (Tree Star, Inc.). Where required, a fixed number of reference beads (Invitrogen) were added per sample. The 10-μm latex beads were distinguished from cells by sideward scatter/forward scatter characteristics. Cell and bead numbers were determined by flow cytometry. Absolute cell numbers in the sample were calculated based on the determined cell/bead ratio and the known number of used beads and sample volume.

Flow cytometry analysis for thymocyte subsets. Thymus suspension cells were stained with a lineage marker mix consisting of biotinylated antibodies (Table S1) against CD19, B220, CD3, CD4, CD8, Gr-1, CD11c, CD11b, Ter119, NK1.1, and γ/δTCR, and were detected by PE-Cy7– or PE-Cy5–conjugated streptavidin (SA). Resolving DN subset distribution was achieved by additional staining for CD25 and CD44 antibodies. For ETP analysis, cells were furthermore stained with Sca-1 and cKit antibodies. For mature thymocyte subset analysis, cells were stained with CD4, CD8, CD24, biotinylated L-selectin (detected with PE-Cy5–SA), Qa-2, and CD69 antibodies.

Analysis and sorting of thymic endothelial and epithelial cells. For sorting, individual thymi were successively digested in 0.2 mg/ml collagenase and 0.2 mg/ml collagenase/dispase (Roche) in RPMI 1640 containing 0.02 mg/ml DNase (Sigma-Aldrich) at 37°C, washed, and filtered through a 100-μm mesh (Thermo Fisher Scientific), as previously described (48). Cells were enriched for stromal and endothelial cells by density centrifugation on a discontinuous Percoll gradient (GE Healthcare), as previously described (bottom layer δ = 1.115 g/ml; middle layer δ =1.06 g/ml; top layer = PBS) (49). Cells recovered from the upper interface were washed and stained with antibodies against CD45, CD31, CD144, G8.8, and Ly51. Cells were negatively gated on CD45; medullary epithelial cells were defined as $CD45^-G8.8^+$, $Ly51^{int}$; cortical epithelial cells were defined as $CD45^-G8.8^+$, $Ly51^{hi}$; and endothelial cells were defined as $CD45^-CD31^+$, $CD144^+$ positive cells (50). Cells were sorted on a FACSVantage and directly sorted into TRIzol LS (Invitrogen) for RNA extraction. For analysis of stromal and endothelial cell numbers, thymi were gently squeezed between two frosted glass slides and agitated in RPMI 1640 for 30 min, replacing the supernatant every 10 min. Thymic tissues were then subjected to enzymatic digestion, as described, to obtain a single-cell suspension. Cells were collected, washed, filtered through a 100-μm mesh, and resuspended in 1 ml of staining buffer containing a fixed number of reference beads to allow for calculation of absolute cell numbers (see Flow cytometry and cell sorting). Cells were stained with the antibodies listed and were analyzed using a LSRII flow cytometer.

Analysis of P-selectin protein expression on thymic endothelial cells. Single-cell suspensions from thymi, obtained as described, were stained with antibodies against CD45, P-selectin, CD31, and CD144, and were analyzed by flow cytometry. Forward and sideward light scatter settings were adjusted to exclude dead cells and platelets. The cells were negatively gated on CD45 to exclude hematopoietic cells and were positively gated for the endothelial markers CD31 and CD144. DP cells were analyzed for the frequency of high P-selectin–expressing cells, thereby excluding possible skewing of the results by different thymic size and relative endothelial content.

Short-term receptivity. Short-tern receptivity was determined by i.v. injection of fluorescent-labeled cells, as previously described (3). In brief, WT bone marrow cells were labeled with 2.5 μM CFSE (Invitrogen) for 5 min at room temperature in HBSS. After staining, 40 million cells were i.v. injected into a nonirradiated recipient. 24 h after injection, recipients were sacrificed, bled, and perfused. Thymi were removed, weighed, and mechanically dissociated to obtain single-cell suspensions, as described in Tissue extraction. Blood samples were treated as described in Blood cell count by flow cytometry. Thymic cell suspensions were stained with lineage markers, as described. After staining, cells were resuspended in 1 ml of staining buffer containing 10^5 reference beads (see Flow cytometry and cell sorting)

Sorting and i.v. injection of TN1–3 subsets. Cell suspensions from up to 8–10 thymi were pooled and labeled with the described lineage marker mix. Lineage marker–positive cells were depleted with SA-coupled magnetic beads using the "depletes" program on an AutoMacs system (all from Miltenyi Biotec). Lineage marker–negative cells were stained with antibodies against CD25 and CD44, and were FACS sorted on a FACSVantage. TN1 ($CD44^+$, $CD25^-$), TN2 ($CD44^+$, $CD25^+$), and TN3 ($CD44^-$, $CD25^+$) cells were collected. The purity of the sorted population was >95%. 5,000 TN cells of each subset together with 10^6 IL-$7R^{-/-}$ splenocytes were i.v. injected into nonirradiated IL-$7R^{-/-}$ recipients. 12d after bone marrow transfer, recipient mice were sacrificed, the thymus and blood were analyzed for donor chimerism, and thymi were additionally analyzed for Psel RNA expression.

Blood cell count by flow cytometry. Mice were bled from the saphenous vein, and 15 μl of peripheral blood was stained with anti-CD4 and -CD8 antibodies. 10^5 reference beads were added per sample. After red blood cell lysis, samples were analyzed by flow cytometry. Cell numbers per microliters of blood were calculated based on the cell/bead ratio (see Flow cytometry and cell sorting).

Real-time PCR. Crudely depleted thymic stromal tissue or sorted cell populations were obtained as described. RNA was extracted using TRIzol solution, according to the manufacturer's instruction. The quality and quantity of total RNA was assessed using a Nanodrop spectrometer (ND-1000; Thermo Fisher Scientific). 1 μg of total RNA was treated with DNase and reverse transcribed using random hexamers and Revert Aid H Minus M-MuLV reverse transcription (all from Fermentas), according to manufacturer's instructions. Gene expression was quantified using the primers/probes listed in Table S2. qrtPCR reactions were performed using TaqMan gene expression or SYBR green PCR master mix and run on a real-time PCR system (HT7900; all from Applied Biosystems). Relative mRNA expression ratios were calculated using the 7000 SDS relative quantification software (Applied Biosystems) or the REST software tool (51), as previously described.

Adoptive transfer. Lymph node cell suspensions from CD45.1 congenic mice were either directly injected into recipients or enriched for T or B cells by negative depletion using anti–rat IgG–coupled magnetic beads (Invitrogen). For T cell enrichment, cells were labeled with rat IgG antibodies against mouse CD19, MHC II, CD11b, and Gr-1, and were subsequently negatively depleted using anti–rat IgG–coupled magnetic beads. Accordingly, B cells were enriched from spleen suspension cells using rat IgG antibodies against mouse CD43, CD11b, MHC II, CD3, and Gr-1. Purities of target populations assessed by flow cytometry were generally >90%. 20×10^6 cells in HBSS were injected i.v. into recipients (CD45.2). 3 d after adoptive transfer, one cohort of recipient mice was analyzed for donor chimerism (CD45.1), S1P level, and thymic P-selectin expression. The other cohort received a bone marrow transplant from a CD45.1/2 congenic donor to test for thymic receptivity. Thymic chimerism was assessed 3 wk after bone marrow transfer by flow cytometry.

S1P measurement: LC-MS/MS. S1P levels in blood plasma and lymphoid tissues were assessed by LC-MS/MS, as previously described (35). In brief, platelet-poor plasma was obtained from blood drawn by cardiac puncture. The plasma samples were diluted with acetonitrile to a final concentration of 20%. The thymus, six lymph nodes, and spleen were homogenized in 4× the volume (assuming a tissue density of 1 g/ml) of 80% acetonitrile. All samples were processed together with 60 ng/ml of internal standard (isotope-labeled S1P, D-erythro-sphingosine-1-phosphate-$^{13}C_2D_2$; Toronto Research Chemicals). After centrifugation, supernatants were analyzed on a hybrid linear ion trap LC-MS/MS system (Q Trap; Applied Biosystems) coupled to an HPLC system (LC Packings) via a Turbo Ion Spray source (Applied Biosystems). Sample separation was performed over a 1 × 50 mm ZORBAX Eclipse XDB-C18 MicroBore column (particle size = 3.5 μm; Agilent Technologies) at the flow rate of 0.2 ml/min using the following gradient: wash column with a mixture of 50% A (water/methanol/acetic acid [69:30:1 vol/vol/vol] containing 5 mM ammonium acetate) and 50% B (methanol/acetic acid [99:1 vol/vol] containing 5 mM ammonium acetate) for 2 min, then apply a linear gradient to 100% B over 4 min, hold 100% B for 2 min, and reequilibrate column with 50% B for 2 min. For the detection of both S1P and internal standard, the Q Trap instrument was operated in positive mode with the ion spray voltage set at 5,000 V and the source temperature set at 400°C. Other MS/MS parameter settings, such as declustering potential and collision energy, were optimized for S1P and internal standard, respectively. The elution of S1P and internal standard were monitored using the multiple reaction monitoring (MRM) mode. The MRM transition (Q1/Q3) settings for S1P and internal standard were 380/264.2 and 384/268.2, respectively. Data were acquired and processed using Analyst 1.4.2 software (Applied Biosystems).

Intrathymic FITC labeling. Intrathymic FITC labeling was performed as previously described (52). In brief, 10 μl of a 2-mg/ml FITC (Sigma-Aldrich) solution in PBS was directly injected into each thymic lobe of anesthetized mice using a Stepper (Tridek). The incision was closed with surgical clips, and mice were sacrificed 36 h after FITC injection. Numbers of $FITC^+CD4^+Lsel^+$ and $FITC^+CD8^+Lsel^+$ positive cells were determined in

thymi, peripheral lymph nodes, and spleens by flow cytometry. Labeling efficiency of thymocytes was, on average, 76%.

Intrathymic bone marrow injection. Intrathymic bone marrow injection was performed as previously described (2). Two million WT bone marrow cells in 10 µl RPMI 1640 were injected into each thymic lobe of anesthetized mice using a Tridek Stepper. 10–14 d after injection, chimerism was assessed by flow cytometry.

TREC analysis. Assessment of TRECs was performed as previously described (53). In brief, T cells from spleens were labeled with biotinylated anti-CD4 and -CD8 antibodies and purified using SA-coupled magnetic beads (Miltenyi Biotec), according to the manufacturer's instruction. After counting, the purified cells were put into TRIzol solution and processed according to the manufacturer's recommendations. After removing the aqueous phase, the DNA was extracted from the remaining interphase and organic phase using back extraction buffer (4 M guanidine thiocyanate, 50 mM sodium citrate, 1 M Tris). After phase separation by centrifugation, the DNA in the aqueous phase was precipitated using isopropanol and the DNA pellet was washed several times with 75% ethanol. The quantity and quality of the DNA was assessed using a Nanodrop spectrometer (ND-1000). Equal amounts of DNA were amplified with primers and detected with a fluorescent-labeled probe (53) using the Probe Master Mix on an LC480 Lightcycler system (both from Roche). Absolute numbers of excision circles were determined using a calibration curve that was produced with known amounts of plasmids (Topo Vector; Invitrogen) containing the target sequence.

FTY720 and DOP treatment. FTY720 (Cayman Chemical) stocks were prepared in DMSO and diluted in vehicle solution (PBS, 0.1% mouse serum) before injection. Mice received 1 mg/kg FTY720 or vehicle alone i.p. for three consecutive days and were analyzed 24 h after the last injection. Mice received 30 mg/liter DOP (4′deoxypyridoxine; Sigma-Aldrich) in drinking water with 10 g/liter glucose for 3 d (20). After FTY720 or DOP treatment, one cohort was sacrificed to analyze thymic P-selectin RNA expression, S1P level, and thymocyte subset distribution. The second cohort received a congenic bone marrow transplant to test for thymic receptivity, as described. Thymic chimerism was assessed 3 wk after bone marrow injection.

Bone marrow transfer. Bone marrow was extracted from respective congenic mice by flushing femurs and tibias with RPMI 1640, 2% FCS, 2 mM EDTA. After red blood cell lysis, 2×10^6 cells in HBSS were injected i.v. into recipients. 3 wk later, thymi, lymph nodes, and spleens were harvested and analyzed for chimerism based on congenic markers (CD45.1 and CD45.2).

In vivo T cell depletion. In vivo T cell depletion was performed by i.p. injection of 0.5 mg anti-CD4 and -CD8 antibodies in PBS. Control mice received PBS only. After 24 h, mice were sacrificed to analyze peripheral T cell numbers, P-selectin RNA level, and S1P level. For testing thymic TCP receptivity, mice received 2×10^6 congenic bone marrow cells 2 d after antibody injection. Thymic chimerism was assessed 3 wk after bone marrow transfer using flow cytometry.

S1P dose–response using the bend.3 endothelial cell line. The mouse endothelial cell line bend.3 (American Type Culture Collection), previously described to express P-selectin and S1PR1 and S1PR2 (54, 55), was cultured in high-glucose DMEM containing 1 mM sodium pyruvate, 0.1 mM of nonessential amino acids, 1,000 U penicillin/streptomycin, and 10% FCS (all from Invitrogen). For the dose–response assay, 50,000 bend.3 cells seeded per well of a 24-well plate (BD) were allowed to adhere overnight, washed several times with serum-free media containing 4% of fatty acid–free BSA (EMD). Cells were cultured for 12 h in serum-free media (+4% of fatty acid–free BSA) containing S1P (Cayman Chemical) at the indicated concentration. Control cells were maintained in serum-free media (+4% of fatty acid–free BSA). Cells were lysed using TRIzol and RNA was extracted according to the manufacturer's instructions (see Real-time PCR).

Statistics. Data are presented as mean values and error bars are presented as SEM. The statistical significance of the data was assessed using an unpaired, two-tailed Student's *t* test (*, $P < 0.05$; **, $P < 0.01$; ***, $P < 0.001$). Statistics were calculated using the SPSS 16 statistics software for Macintosh.

Online supplemental material. Fig. S1 shows thymic cellularity of the mouse strains used. Fig. S2 shows the time course of P-selectin RNA expression in spleens of WT, C2GnT1$^{-/-}$, and PSGL-1$^{-/-}$ mice. Fig. S3 shows the results of TN1, TN2, and TN3 injections into IL-7R$^{-/-}$ mice. Fig. S4 shows the RNA level of S1P1R, KLF2, and S1P-lyase in thymocyte subsets of WT, C2GnT1$^{-/-}$, and PSGL-1$^{-/-}$ mice. Fig. S5 shows the efficacy of peripheral T cell depletion in WT mice or boost in PSGL-1$^{-/-}$ mice. Fig. S6 shows the efficacy of FTY720 treatment. Fig. S7 shows the efficacy of DOP treatment. Table S1 shows the primers used, and Table S2 shows the antibodies used. Online supplemental material is available at http://www.jem.org/cgi/content/full/jem.20082502/DC1.

We thank D.A. Carlow for helpful discussions and for critically reading the manuscript; L. Yi, Y. Even, M. Williams, and A. Johnson for technical assistance; and J. Marth for C2GnT1$^{-/-}$ mice.

This work was supported by grants MOP-81382 (to F.M.V. Rossi), and MOP-82867 and MOP-77552 (to H.J. Ziltener) from the Canadian Institutes of Health Research (CIHR). K. Gossens was the recipient of a CIHR Transplantation Fellowship, and S. Naus was supported by a fellowship from the Heart and Stroke Society.

The authors have no conflicting financial interests.

Submitted: 5 November 2008
Accepted: 23 February 2009

REFERENCES

1. Donskoy, E., and I. Goldschneider. 1992. Thymocytopoiesis is maintained by blood-borne precursors throughout postnatal life. A study in parabiotic mice. *J. Immunol.* 148:1604–1612.
2. Foss, D.L., E. Donskoy, and I. Goldschneider. 2001. The importation of hematogenous precursors by the thymus is a gated phenomenon in normal adult mice. *J. Exp. Med.* 193:365–374.
3. Rossi, F.M., S.Y. Corbel, J.S. Merzaban, D.A. Carlow, K. Gossens, J. Duenas, L. So, L. Yi, and H.J. Ziltener. 2005. Recruitment of adult thymic progenitors is regulated by P-selectin and its ligand PSGL-1. *Nat. Immunol.* 6:626–634.
4. Scimone, M.L., I. Aifantis, I. Apostolou, H. von Boehmer, and U.H. von Andrian. 2006. A multistep adhesion cascade for lymphoid progenitor cell homing to the thymus. *Proc. Natl. Acad. Sci. USA.* 103:7006–7011.
5. Ellies, L.G., S. Tsuboi, B. Petryniak, J.B. Lowe, M. Fukuda, and J.D. Marth. 1998. Core 2 oligosaccharide biosynthesis distinguishes between selectin ligands essential for leukocyte homing and inflammation. *Immunity.* 9:881–890.
6. Prockop, S.E., and H.T. Petrie. 2004. Regulation of thymus size by competition for stromal niches among early T cell progenitors. *J. Immunol.* 173:1604–1611.
7. Bhandoola, A., H. von Boehmer, H.T. Petrie, and J.C. Zuniga-Pflucker. 2007. Commitment and developmental potential of extrathymic and intrathymic T cell precursors: plenty to choose from. *Immunity.* 26:678–689.
8. Foss, D.L., E. Donskoy, and I. Goldschneider. 2002. Functional demonstration of intrathymic binding sites and microvascular gates for prothymocytes in irradiated mice. *Int. Immunol.* 14:331–338.
9. Shortman, K., and L. Wu. 1996. Early T lymphocyte progenitors. *Annu. Rev. Immunol.* 14:29–47.
10. McCaughtry, T.M., M.S. Wilken, and K.A. Hogquist. 2007. Thymic emigration revisited. *J. Exp. Med.* 204:2513–2520.
11. Boursalian, T.E., J. Golob, D.M. Soper, C.J. Cooper, and P.J. Fink. 2004. Continued maturation of thymic emigrants in the periphery. *Nat. Immunol.* 5:418–425.
12. Petrie, H.T., and J.C. Zuniga-Pflucker. 2007. Zoned out: functional mapping of stromal signaling microenvironments in the thymus. *Annu. Rev. Immunol.* 25:649–679.

13. Xia, P., J.R. Gamble, K.A. Rye, L. Wang, C.S. Hii, P. Cockerill, Y. Khew-Goodall, A.G. Bert, P.J. Barter, and M.A. Vadas. 1998. Tumor necrosis factor-alpha induces adhesion molecule expression through the sphingosine kinase pathway. *Proc. Natl. Acad. Sci. USA.* 95:14196–14201.
14. Sanna, M.G., S.K. Wang, P.J. Gonzalez-Cabrera, A. Don, D. Marsolais, M.P. Matheu, S.H. Wei, I. Parker, E. Jo, W.C. Cheng, et al. 2006. Enhancement of capillary leakage and restoration of lymphocyte egress by a chiral S1P1 antagonist in vivo. *Nat. Chem. Biol.* 2:434–441.
15. Lee, M.J., S. Thangada, K.P. Claffey, N. Ancellin, C.H. Liu, M. Kluk, M. Volpi, R.I. Sha'afi, and T. Hla. 1999. Vascular endothelial cell adherens junction assembly and morphogenesis induced by sphingosine-1-phosphate. *Cell.* 99:301–312.
16. Matsushita, K., C.N. Morrell, and C.J. Lowenstein. 2004. Sphingosine 1-phosphate activates Weibel-Palade body exocytosis. *Proc. Natl. Acad. Sci. USA.* 101:11483–11487.
17. Pan, J., L. Xia, L. Yao, and R.P. McEver. 1998. Tumor necrosis factor-alpha- or lipopolysaccharide-induced expression of the murine P-selectin gene in endothelial cells involves novel kappaB sites and a variant activating transcription factor/cAMP response element. *J. Biol. Chem.* 273:10068–10077.
18. Rivera, J., R.L. Proia, and A. Olivera. 2008. The alliance of sphingosine-1-phosphate and its receptors in immunity. *Nat. Rev. Immunol.* 8:753–763.
19. Brinkmann, V. 2007. Sphingosine 1-phosphate receptors in health and disease: mechanistic insights from gene deletion studies and reverse pharmacology. *Pharmacol. Ther.* 115:84–105.
20. Schwab, S.R., J.P. Pereira, M. Matloubian, Y. Xu, Y. Huang, and J.G. Cyster. 2005. Lymphocyte sequestration through S1P lyase inhibition and disruption of S1P gradients. *Science.* 309:1735–1739.
21. Schnell, F.J., A.L. Zoller, S.R. Patel, I.R. Williams, and G.J. Kersh. 2006. Early growth response gene 1 provides negative feedback to inhibit entry of progenitor cells into the thymus. *J. Immunol.* 176:4740–4747.
22. Lai, A.Y., and M. Kondo. 2007. Identification of a bone marrow precursor of the earliest thymocytes in adult mouse. *Proc. Natl. Acad. Sci. USA.* 104:6311–6316.
23. Schwarz, B.A., A. Sambandam, I. Maillard, B.C. Harman, P.E. Love, and A. Bhandoola. 2007. Selective thymus settling regulated by cytokine and chemokine receptors. *J. Immunol.* 178:2008–2017.
24. Goldschneider, I. 2006. Cyclical mobilization and gated importation of thymocyte progenitors in the adult mouse: evidence for a thymus-bone marrow feedback loop. *Immunol. Rev.* 209:58–75.
25. Jotereau, F., F. Heuze, V. Salomon-Vie, and H. Gascan. 1987. Cell kinetics in the fetal mouse thymus: precursor cell input, proliferation, and emigration. *J. Immunol.* 138:1026–1030.
26. Cummins, A.G., and F.M. Thompson. 1997. Postnatal changes in mucosal immune response: a physiological perspective of breast feeding and weaning. *Immunol. Cell Biol.* 75:419–429.
27. Hobson, B., and J. Denekamp. 1984. Endothelial proliferation in tumours and normal tissues: continuous labelling studies. *Br. J. Cancer.* 49:405–413.
28. Gray, D., J. Abramson, C. Benoist, and D. Mathis. 2007. Proliferative arrest and rapid turnover of thymic epithelial cells expressing Aire. *J. Exp. Med.* 204:2521–2528.
29. Irla, M., S. Hugues, J. Gill, T. Nitta, Y. Hikosaka, I.R. Williams, F.X. Hubert, H.S. Scott, Y. Takahama, G.A. Hollander, and W. Reith. 2008. Autoantigen-specific interactions with CD4+ thymocytes control mature medullary thymic epithelial cell cellularity. *Immunity.* 29:451–463.
30. Van Parijs, L., and A.K. Abbas. 1998. Homeostasis and self-tolerance in the immune system: turning lymphocytes off. *Science.* 280:243–248.
31. Veerman, K.M., M.J. Williams, K. Uchimura, M.S. Singer, J.S. Merzaban, S. Naus, D.A. Carlow, P. Owen, J. Rivera-Nieves, S.D. Rosen, and H.J. Ziltener. 2007. Interaction of the selectin ligand PSGL-1 with chemokines CCL21 and CCL19 facilitates efficient homing of T cells to secondary lymphoid organs. *Nat. Immunol.* 8:532–539.
32. Siehler, S., Y. Wang, X. Fan, R.T. Windh, and D.R. Manning. 2001. Sphingosine 1-phosphate activates nuclear factor-kappa B through Edg receptors. Activation through Edg-3 and Edg-5, but not Edg-1, in human embryonic kidney 293 cells. *J. Biol. Chem.* 276:48733–48739.
33. Baldwin, A.S., Jr. 1996. The NF-kappa B and I kappa B proteins: new discoveries and insights. *Annu. Rev. Immunol.* 14:649–683.
34. Venkataraman, K., Y.M. Lee, J. Michaud, S. Thangada, Y. Ai, H.L. Bonkovsky, N.S. Parikh, C. Habrukowich, and T. Hla. 2008. Vascular endothelium as a contributor of plasma sphingosine 1-phosphate. *Circ. Res.* 102:669–676.
35. Pappu, R., S.R. Schwab, I. Cornelissen, J.P. Pereira, J.B. Regard, Y. Xu, E. Camerer, Y.W. Zheng, Y. Huang, J.G. Cyster, and S.R. Coughlin. 2007. Promotion of lymphocyte egress into blood and lymph by distinct sources of sphingosine-1-phosphate. *Science.* 316:295–298.
36. Hannun, Y.A., and L.M. Obeid. 2008. Principles of bioactive lipid signalling: lessons from sphingolipids. *Nat. Rev. Mol. Cell Biol.* 9:139–150.
37. Nageh, M.F., E.T. Sandberg, K.R. Marotti, A.H. Lin, E.P. Melchior, D.C. Bullard, and A.L. Beaudet. 1997. Deficiency of inflammatory cell adhesion molecules protects against atherosclerosis in mice. *Arterioscler. Thromb. Vasc. Biol.* 17:1517–1520.
38. Yatomi, Y. 2008. Plasma sphingosine 1-phosphate metabolism and analysis. *Biochim. Biophys. Acta.* 1780:606–611.
39. Deutschman, D.H., J.S. Carstens, R.L. Klepper, W.S. Smith, M.T. Page, T.R. Young, L.A. Gleason, N. Nakajima, and R.A. Sabbadini. 2003. Predicting obstructive coronary artery disease with serum sphingosine-1-phosphate. *Am. Heart J.* 146:62–68.
40. Ammit, A.J., A.T. Hastie, L.C. Edsall, R.K. Hoffman, Y. Amrani, V.P. Krymskaya, S.A. Kane, S.P. Peters, R.B. Penn, S. Spiegel, and R.A. Panettieri Jr. 2001. Sphingosine 1-phosphate modulates human airway smooth muscle cell functions that promote inflammation and airway remodeling in asthma. *FASEB J.* 15:1212–1214.
41. Kitano, M., T. Hla, M. Sekiguchi, Y. Kawahito, R. Yoshimura, K. Miyazawa, T. Iwasaki, H. Sano, J.D. Saba, and Y.Y. Tam. 2006. Sphingosine 1-phosphate/sphingosine 1-phosphate receptor 1 signaling in rheumatoid synovium: regulation of synovial proliferation and inflammatory gene expression. *Arthritis Rheum.* 54:742–753.
42. Massberg, S., P. Schaerli, I. Knezevic-Maramica, M. Kollnberger, N. Tubo, E.A. Moseman, I.V. Huff, T. Junt, A.J. Wagers, I.B. Mazo, and U.H. von Andrian. 2007. Immunosurveillance by hematopoietic progenitor cells trafficking through blood, lymph, and peripheral tissues. *Cell.* 131:994–1008.
43. Kimura, T., A.M. Boehmler, G. Seitz, S. Kuci, T. Wiesner, V. Brinkmann, L. Kanz, and R. Mohle. 2004. The sphingosine 1-phosphate receptor agonist FTY720 supports CXCR4-dependent migration and bone marrow homing of human CD34+ progenitor cells. *Blood.* 103:4478–4486.
44. Bandhuvula, P., and J.D. Saba. 2007. Sphingosine-1-phosphate lyase in immunity and cancer: silencing the siren. *Trends Mol. Med.* 13:210–217.
45. Aoki, S., Y. Yatomi, M. Ohta, M. Osada, F. Kazama, K. Satoh, K. Nakahara, and Y. Ozaki. 2005. Sphingosine 1-phosphate-related metabolism in the blood vessel. *J. Biochem.* 138:47–55.
46. Yatomi, Y., T. Ohmori, G. Rile, F. Kazama, H. Okamoto, T. Sano, K. Satoh, S. Kume, G. Tigyi, Y. Igarashi, and Y. Ozaki. 2000. Sphingosine 1-phosphate as a major bioactive lysophospholipid that is released from platelets and interacts with endothelial cells. *Blood.* 96:3431–3438.
47. Vachino, G., X.J. Chang, G.M. Veldman, R. Kumar, D. Sako, L.A. Fouser, M.C. Berndt, and D.A. Cumming. 1995. P-selectin glycoprotein ligand-1 is the major counter-receptor for P-selectin on stimulated T cells and is widely distributed in non-functional form on many lymphocytic cells. *J. Biol. Chem.* 270:21966–21974.
48. Gray, D.H., A.L. Fletcher, M. Hammett, N. Seach, T. Ueno, L.F. Young, J. Barbuto, R.L. Boyd, and A.P. Chidgey. 2008. Unbiased analysis, enrichment and purification of thymic stromal cells. *J. Immunol. Methods.* 329:56–66.
49. Nedjic, J., M. Aichinger, J. Emmerich, N. Mizushima, and L. Klein. 2008. Autophagy in thymic epithelium shapes the T-cell repertoire and is essential for tolerance. *Nature.* 455:396–400.
50. Venanzi, E.S., D.H. Gray, C. Benoist, and D. Mathis. 2007. Lymphotoxin pathway and Aire influences on thymic medullary epithelial cells are unconnected. *J. Immunol.* 179:5693–5700.
51. Pfaffl, M.W., G.W. Horgan, and L. Dempfle. 2002. Relative expression software tool (REST) for group-wise comparison and statistical

analysis of relative expression results in real-time PCR. *Nucleic Acids Res.* 30:e36.
52. Scollay, R.G., E.C. Butcher, and I.L. Weissman. 1980. Thymus cell migration. Quantitative aspects of cellular traffic from the thymus to the periphery in mice. *Eur. J. Immunol.* 10:210–218.
53. Sempowski, G.D., M.E. Gooding, H.X. Liao, P.T. Le, and B.F. Haynes. 2002. T cell receptor excision circle assessment of thymopoiesis in aging mice. *Mol. Immunol.* 38:841–848.
54. Pan, J., L. Xia, and R.P. McEver. 1998. Comparison of promoters for the murine and human P-selectin genes suggests species-specific and conserved mechanisms for transcriptional regulation in endothelial cells. *J. Biol. Chem.* 273:10058–10067.
55. Mulders, A.C., M.C. Hendriks-Balk, M.J. Mathy, M.C. Michel, A.E. Alewijnse, and S.L. Peters. 2006. Sphingosine kinase-dependent activation of endothelial nitric oxide synthase by angiotensin II. *Arterioscler. Thromb. Vasc. Biol.* 26:2043–2048.